

New *para-para* Stilbenophanes: Synthesis by McMurry Coupling, Conformational Analysis and Inhibition of Tubulin Polymerisation

Raquel Álvarez, Vilmarí López, Carmen Mateo, Manuel Medarde,* and Rafael Peláez*^[a]

Abstract: The synthesis of a new family of methoxy-substituted [2.7]- and [2.8]paracyclophanes linked by 3-oxapentamethylene-1,5-dioxy and hexamethylene-1,6-dioxy bridges has been carried out by using the McMurry methodology. Related indole compounds were also synthesised. Olefin-to-diol ratios depended on the bridge length, the structure of the aromatic ring and the reaction conditions. Mac-

rocyclisation, the methoxy substituents and the presence of a rigid indole moiety restricted the conformational equilibria, as observed by NMR spec-

trosopy and according to theoretical calculations. The synthesised compounds display micromolar tubulin polymerisation inhibitory activity. The conformational implications on the tubulin polymerisation inhibitory activity derived from the macrocyclisation when compared with combretastatins, closely related stilbenes, are also discussed.

Keywords: combretastatin analogues • conformation analysis • cyclophanes • structure–activity relationships • tubulin polymerization inhibition

Introduction

Stilbenes are widely studied substructures in organic chemistry owing to their presence in a large number of organic compounds with applications in different fields. One point of interest is the biological activity displayed by stilbene derivatives,^[1] as in the case of the anticancer agents combretastatins^[2] and resveratrol.^[3] Considerable efforts have been invested in the preparation of analogues of these compounds to unveil the structure–activity relationships and improve the pharmacological profile by increasing the activity and selectivity.^[4] In this sense, the prodrug combretastatin A-4 phosphate^[5] appears to be a good drug candidate, owing to its vascular disrupting activity and adequate water solubility. Currently, it is in phase II/III clinical trials for the treatment of anaplastic thyroid cancer and solid tumours.^[6]

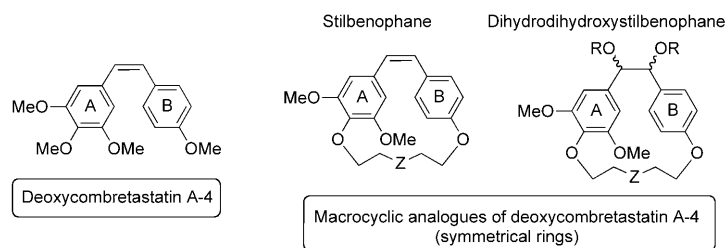
Conformational restriction is a method for exploring the influence of molecular geometry on physicochemical and biological properties^[7] that can be achieved by several approaches, including the macrocyclisation of open-chain active models.^[8] This has been applied to diverse types of compounds,^[9] such as bisindole derivatives,^[10] and it has recently been used as a tool for a systematic search for new

active derivatives in different cell assays.^[11] Although it is a very interesting approach for modulating the activity–selectivity of analogues based on highly potent lead compounds, it has not yet been applied to active stilbenes and we have only recently published preliminary work addressing this issue.^[12] The compounds designed for this purpose are stilbene and dihydrostilbene derivatives conformationally blocked by the formation of macrocyclic structures, which can be classified as cyclophanes,^[13] in general, or stilbenophanes, in particular.^[14] Stilbenophanes have recently received renewed interest by Rajakumar's group,^[15] who have studied the potential applicability and that of related indolophanes^[16] in supramolecular chemistry.

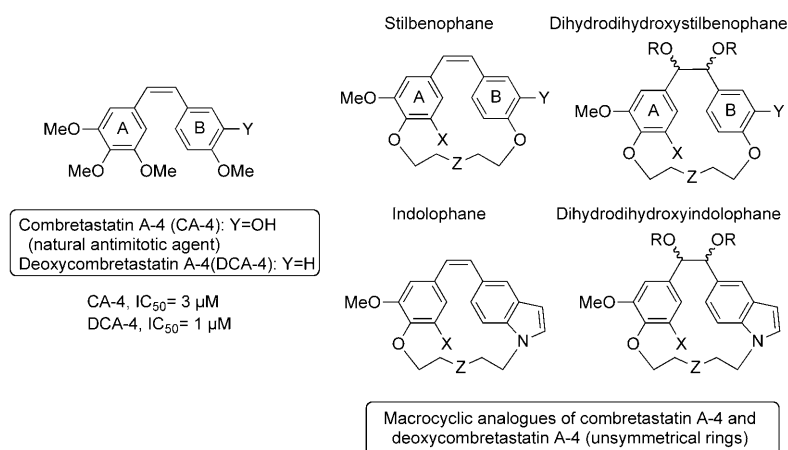
The synthetic approach to these stilbene and dihydrostilbene cyclophanes can be planned through different approaches; intramolecular McMurry coupling is the preferred tool to produce the macrocyclisation step. During our research into new antimitotic agents based on natural products,^[17] we described the application of the McMurry methodology^[12a] to the synthesis of a new family of doubly symmetric (two symmetric benzene rings) stilbenophanes based on deoxycombretastatin A-4 (Scheme 1),^[18] the preparation

[a] Dr. R. Álvarez, Dr. V. López, Dr. C. Mateo, Prof. Dr. M. Medarde, Dr. R. Peláez
Laboratorio de Química Orgánica y Farmacéutica
Facultad de Farmacia. Universidad de Salamanca
Campus Miguel de Unamuno, 37007, Salamanca (Spain)
Fax: (+34) 923-294515
E-mail: pelaez@usal.es
medarde@usal.es

Supporting information for this article is available on the WWW under <http://dx.doi.org/10.1002/chem.201002869>.



Scheme 1. Comparison of the structures of previously described stilbenophanes with deoxycombretastatin A-4.



Scheme 2. Comparison of the structures of synthesised stilbenophanes and related indolophanes with the potent antimittotic agents combretastatin A-4 and deoxycombretastatin A-4.

of some dihydrodihydroxy members of this class of compounds,^[12b,d] and we also reported the results of the biological assays carried out on some of them.^[12c]

Herein, we describe the results obtained upon applying this chemistry to the preparation of macrocyclic analogues of combretastatin A-4 (Scheme 2), differently substituted at the A or B rings, and the conformational analysis of the produced olefins. The conformational equilibria for these compounds are characterised by the coexistence of differently preferred conformations in rapid or intermediate exchange. The existence of favoured conformations and the dynamics of the conformational equilibria of these compounds can produce a noticeable effect on their interaction with their targets and on their cytotoxic activity. A better knowledge of the spatial arrangement adopted by these molecules can facilitate the design of new analogues with improved potency in comparison with the stilbenophanes and indolophanes already obtained.^[12c]

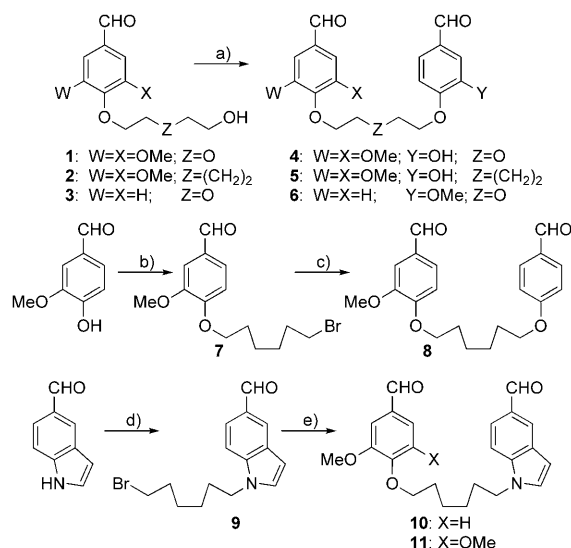
The detailed description and conformational analysis of diols and their derivatives will be published elsewhere. The successful synthesis of unsymmetrical stilbenophanes and indolophanes opens the possibility of studying the applicability of these fascinating compounds (in terms of their conformational mobility) in supramolecular and medicinal chemistry.

Results and Discussion

The synthesis of the designed molecules was carried out according to the approaches described in Schemes 3 and 4: two consecutive alkylations of suitable phenolic (indolic) aldehydes with the required reactive linker moiety produced the intermediate dialdehydes (Scheme 3), which were subjected to McMurry internal coupling (at room temperature or under reflux (Scheme 4)). The alkylation processes were performed by the Mitsunobu^[19] or catalysed phase-transfer^[20] methodologies, depending on the particular cases and

the linker structure. The use of polymer-bound triphenylphosphine in the Mitsunobu reaction is recommended to avoid the presence of phosphine oxides in the coupling step mediated by titanium,^[21] because small amounts of phosphorous materials elicit a decrease in the yields or the absence of isolable reaction products.

The McMurry olefinations^[22] and pinacol couplings^[23] produced olefins, diols or mixtures of both types of compounds, depending on the specific condi-

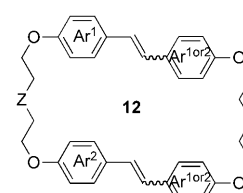


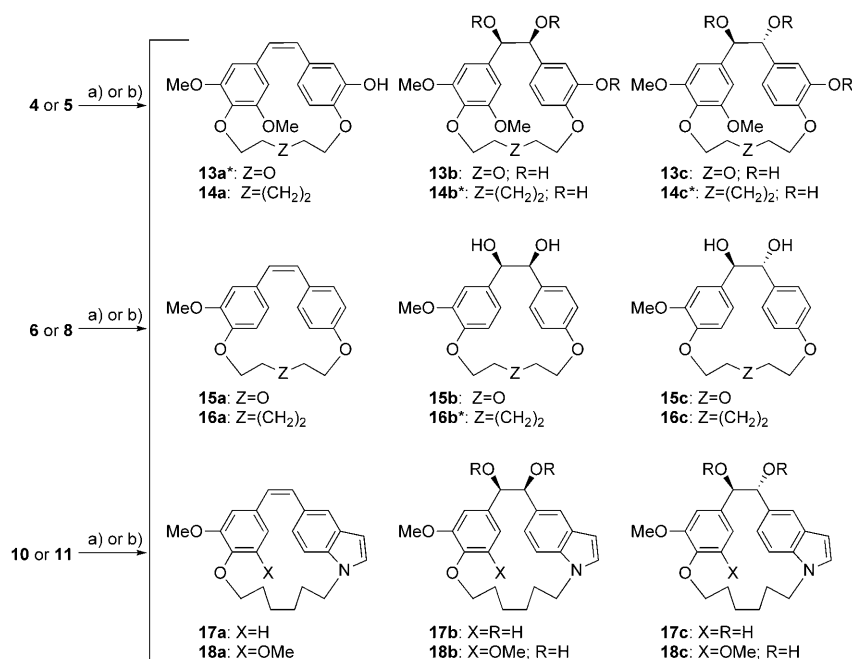
Scheme 3. Synthesis of intermediate dialdehydes **1**, **2** and **3**.^[12d] Reagents and conditions: a) 1) PPh₃ resin, aldehyde, CH₂Cl₂, RT, 1–3 h; 2) di(*tert*-butyl) azodicarboxylate (DBAD)/diisopropyl azodicarboxylate (DIAD), RT, 48 h; b) NaOH, 1,6-dibromohexane, CH₂Cl₂/H₂O 1:1, Bu₄NF, RT, 48 h; c) *p*-hydroxybenzaldehyde, K₂CO₃, dry DMF, 60 °C, 48 h, Ar; d) NaOH, 1,6-dibromohexane, CH₂Cl₂, Bu₄NSO₄H, RT, 24 h; e) vanillin or syringaldehyde, K₂CO₃, dry DMF, 70 °C, 48 h, Ar.

tions and structures. Although the yields varied from moderate to high, most of the olefins were isolated in sufficient quantities to characterise and assay them (Scheme 4).

Under the employed conditions, no dimeric products (as represented by the general structure **12**) were isolated in any of the syntheses carried out, but they were detected as minor products from dialdehyde **8**.

The product ratios (as estimated by ¹H NMR spectroscopy) for each crude reaction





Scheme 4. Reagents and conditions: a) 1) TiCl_4 ·THF (97%), Zn, dry THF, 0 °C, refluxed for 30 min; 2) dialdehyde, dry THF, 2–24 h, reflux; b) same as a) but 0 °C or RT, 5–24 h. Products marked with * were not isolated after chromatography.

Table 1. Results of McMurry cyclisation reactions in Scheme 4, produced under the conditions shown.

Entry	Starting material	Reaction conditions	Crude yield [%]	Product (ratio) ^[a]	Olefin (yield [%]) ^[b]
1	4	5 h; reflux	94	13b/13c (1/1)	–
2	5	23 h; reflux	complex mixture	– ^[c]	14a (40)
3	5	5 h; 0 °C	100	14b/14c (1/3)	–
4	6	24 h; reflux	complex mixture	15a/15b/15c (1/1/2)	15a (15)
5	8	24 h; reflux	complex mixture	– ^[c]	16a (7)
6	8	24 h; RT	complex mixture	– ^[c]	–
7	10	5 h; reflux	97	17a/17b/17c (1/2/2)	17a (10)
8	10	2 h; reflux	70	17a/17b/17c (1/2/2)	17a (7)
9	11	5 h; reflux	100	18a/18b/18c (3/2/1)	18a (30)

[a] Product ratios of the crude mixture were estimated by integration of representative signals in the ^1H NMR spectra of the crude reaction products. [b] Yield obtained after isolation by flash chromatography. [c] Not established by ^1H NMR spectroscopy.

mixture and the isolated yields of the olefins are indicated in Table 1. Olefins (**a**) were always produced under reflux (Table 1, entries 2, 4, 5, 7, 8 and 9), except for compound **4** (Table 1, entry 1), but they were not detected in the crude reaction products when the reactions were carried out at lower temperatures (Table 1, entries 3 (0 °C) and 6 (RT)). Diols (**b**, **c**) were produced at lower temperatures (Table 1, entries 3 and 6), whereas under reflux they were either not detected (Table 1, entries 2 and 5) or were produced in different ratios (Table 1, entries 1, 4, 7, 8 and 9). The results of the McMurry reaction were variable depending on the reaction conditions and substrates employed,^[24] as observed in Table 1.

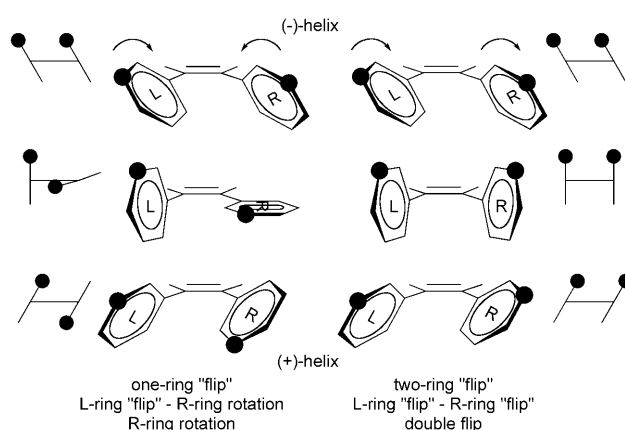
The structures of the olefins were readily established by ^1H NMR spectroscopy, which showed the presence of the *cis* double bond and the usual appearance of only one signal for the chemically equivalent protons at room temperature.

Complete resonance assignments for all of the macrocycles were achieved by 2D NMR spectroscopy (COSY, HMQC, HMBC and ROESY). Diols and their acetates will be studied in depth in forthcoming papers.

Conformational analysis^[25]

Previously studied macrocyclic olefins of this class with two symmetrically substituted phenyl rings were seen to have simple NMR spectra, with signal averaging of the chemically equivalent pairs, both in the ^1H and the ^{13}C NMR spectra.^[12a,b] In that case, the chemical exchange of these nuclei took place readily through helical changes (double flip, see Scheme 5)^[26] that occur without the passage of any of the ring planes through the intra-annular space, represented by the double-bond plane.

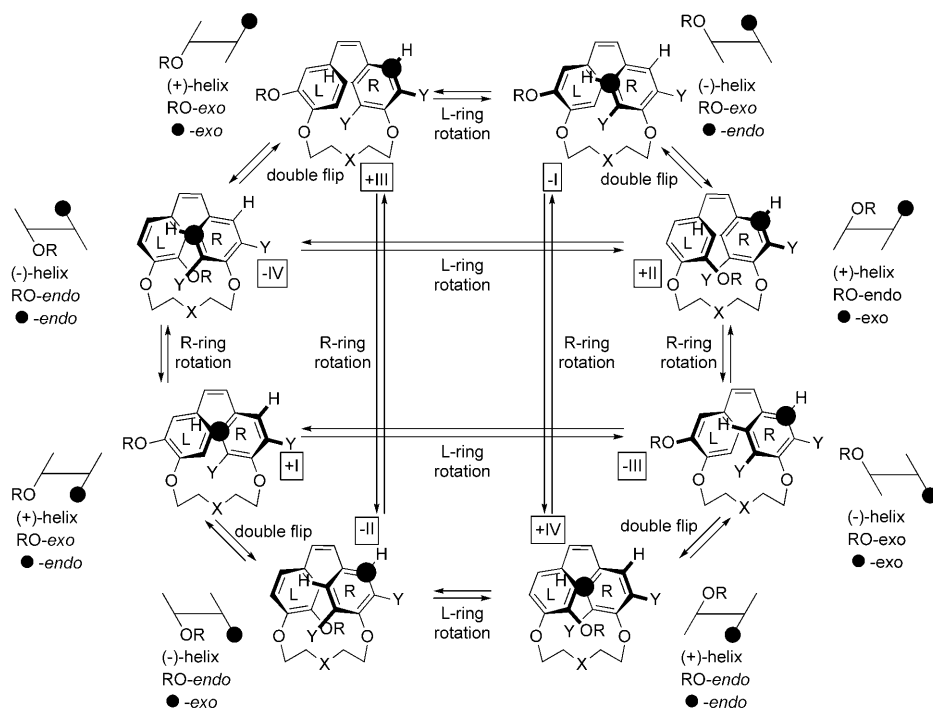
Deeper insight into the conformational equilibria in which these kinds of compounds are involved can be obtained from the compounds described herein, which have at least one non-symmetrically substituted aromatic ring. In each case, a single set of signals is observed



Scheme 5. Definitions and schematic representations of the phenyl ring motions for the stilbene and the associated helicity changes.^[27] Left: one-ring flip and one-ring rotation, which is a disrotatory movement exemplified herein from the (–)-helix (at the top) to the (+)-helix (at the bottom). Right: the two-ring flip, referred to herein as a double flip, is a conrotatory movement.

for compounds with either two non-symmetrical rings (**17a**) or with one symmetrical ring (**14a**, **15a**, **16a** and **18a**). In the case of the latter group, signal averaging of the chemically equivalent nuclei of the symmetrical ring is usually observed. This can only be explained by either the existence of a single set of dominating conformations (see below) or by a conformational exchange involving the passage of ring planes through the intra-annular space.

The relevant conformational classes, as determined by molecular mechanics calculations, are depicted in Scheme 6. The combination of two helical dispositions (+ and -), with



Scheme 6. Conformational equilibria for olefins **14a** ($X=CH_2CH_2$, $R=H$, $Y=OMe$), **15a** ($X=O$, $R=Me$, $Y=H$) and **16a** ($X=CH_2CH_2$, $R=Me$, $Y=H$), with one symmetric ring. A schematic representation is also included that shows the planes of the double bond (horizontal line) and both aromatic rings (vertical lines), together with an indication of the helicity (vertical lines angled from left to right indicate a (-)-helix and from right to left indicate a (+)-helix). Marked positions (●) facilitate the visualisation of their location above or below the double-bond plane.

two different situations for the marked position in each ring (above and below the plane of the double bond), gives rise to $2 \times 2 \times 2 = 8$ conformational populations. Four populations are mirror images of the other four and only differ in their helical disposition, and they are indistinguishable from the NMR spectroscopy point of view. Accordingly, the eight conformations were labelled I to IV preceded by their helical sign to simplify the identification of the pairs of mirror images.

Furthermore, for compounds with one symmetric and one non-symmetric phenyl ring, such as **14a** ($X=CH_2-CH_2$, $R=H$, $Y=OMe$), **15a** ($X=O$, $R=Me$, $Y=H$) and **16a** ($X=CH_2-CH_2$, $R=Me$, $Y=H$), conformations I and III are indistinguishable, but the marked positions are located in differ-

ent surroundings in each case. The same applies for conformations II and IV.

As shown in Scheme 6, rotation of the aromatic rings can interconvert the conformations. Ring rotations (L- for the ring on the left and R- for that on the right) pass the corresponding ring planes through the intra-annular space, while flip movements pass them through the normal to the double-bond plane. Usually, flipping or rotating one aromatic ring causes the other ring to flip, in both cases resulting in a change in helicity (see Scheme 5 for stilbene).^[26,28] One-ring rotation accompanied by one-ring flip (Scheme 5, left; produced by R-ring rotation and L-ring flip) changes the orientation of the marked positions only for the rotating R-ring, from above to below. A two-ring flip (Scheme 5, right) causes no change in their disposition, both still lying above the plane after the helix change. Simultaneous rotation of both rings (zero-ring flip, not drawn) would require an improbable co-planar disposition of both rings. In Scheme 6, the conformations are switched horizontally by rotation of the L-ring (accompanied by R-ring flip); vertically by rotation of the R-ring (accompanied by L-ring flip), and on the external diagonals by double flips. Fast rotation of the R- and/or L-rings through the macrocycle and/or double flips are required for the appearance of chemically

equivalent positions as a single signal in NMR spectra (see Tables 2 and 3).

As stated above, most of the NMR spectra of these macrocyclic olefins display a single set of signals. For **17a**, with two

non-axially symmetric rings, the presence of only one set of signals requires a fast exchange between four populations (I–IV), the presence of a single dominating conformational population, or intermediate situations (e.g., two rapidly exchanging major conformations). For compounds with one axially symmetric ring, such as **14a**, **15a**, **16a** or **18a**, there are only two types of conformational populations that would generate different NMR spectra, namely, $\pm I/\pm III$ and $\pm II/\pm IV$. The presence of a single set of signals in the NMR spectra requires either the prevalence of one of the groups or a fast exchange between individual members of the two groups, as occurs in stilbene. Theoretical calculations suggest that both groups of conformations are of similar stability. Furthermore, the signal averaging usually ob-

Table 2. Independent equilibria remaining if only two motions (as indicated in the upper row) are fast on the NMR spectroscopy timescale.^[a]

Fast L-ring rotation Fast R-ring rotation Slow double flip	Fast R-ring rotation Fast double flip Slow L-ring rotation	Fast L-ring rotation Fast double flip Slow R-ring rotation
$(\pm) \text{I} \longleftrightarrow (\mp) \text{III}$ RO- <i>exo</i> RO- <i>exo</i> ●- <i>endo</i> ●- <i>exo</i> ○- <i>exo</i> ○- <i>endo</i>	$(\pm) \text{I} \longleftrightarrow (\mp) \text{IV}$ RO- <i>exo</i> RO- <i>endo</i> ●- <i>endo</i> ●- <i>endo</i> ○- <i>exo</i> ○- <i>exo</i>	$(\pm) \text{I} \longleftrightarrow (\mp) \text{III}$ RO- <i>exo</i> RO- <i>exo</i> ●- <i>endo</i> ●- <i>exo</i> ○- <i>exo</i> ○- <i>endo</i>
$(\mp) \text{IV} \longleftrightarrow (\pm) \text{II}$ RO- <i>endo</i> RO- <i>endo</i> ●- <i>endo</i> ●- <i>exo</i> ○- <i>exo</i> ○- <i>endo</i>	$(\mp) \text{II} \longleftrightarrow (\pm) \text{III}$ RO- <i>endo</i> RO- <i>exo</i> ●- <i>exo</i> ●- <i>exo</i> ○- <i>endo</i> ○- <i>endo</i>	$(\mp) \text{II} \longleftrightarrow (\pm) \text{IV}$ RO- <i>endo</i> RO- <i>endo</i> ●- <i>exo</i> ●- <i>endo</i> ○- <i>endo</i> ○- <i>exo</i>
RO- <i>endo</i> / RO- <i>exo</i> : averaged ● / ○: averaged	RO- <i>endo</i> / RO- <i>exo</i> : averaged ● / ○: averaged	RO- <i>endo</i> / RO- <i>exo</i> : averaged ● / ○: averaged
one set of signals	one set of signals	one set of signals

[a] The horizontal equilibrium arrows indicate conversions caused by the first fast motion and the vertical ones indicate conversions caused by the second fast motion. The *endo* or *exo* dispositions of the substituent for the trisubstituted L-rings are indicated by RO-*endo/exo* just below the conformation number (I–IV) and the corresponding disposition of chemically equivalent positions (labelled ● and ○) of the symmetrical rings are indicated underneath. The lower row shows an indication of what would be observed in the NMR spectra.

Table 3. Representation of the independent equilibria (separated by dotted lines) remaining if only one motion (as indicated in the upper row) is fast on the NMR timescale.^[a]

Fast L-ring rotation Slow R-ring rotation Slow double flip	Fast R-ring rotation Slow L-ring rotation Slow double flip	Fast double flip Slow R-ring rotation Slow L-ring rotation
$(\pm) \text{I} \longleftrightarrow (\mp) \text{III}$ RO- <i>exo</i> RO- <i>exo</i> ●- <i>endo</i> ●- <i>exo</i> ○- <i>exo</i> ○- <i>endo</i>	$(\pm) \text{I} \longleftrightarrow (\mp) \text{IV}$ RO- <i>exo</i> RO- <i>endo</i> ●- <i>endo</i> ●- <i>endo</i> ○- <i>exo</i> ○- <i>exo</i>	$(\pm) \text{I} \longleftrightarrow (\mp) \text{II}$ RO- <i>exo</i> RO- <i>endo</i> ●- <i>endo</i> ●- <i>exo</i> ○- <i>exo</i> ○- <i>endo</i>
●- <i>endo</i> / ●- <i>exo</i> : averaged ○- <i>exo</i> / ○- <i>endo</i> : averaged	RO- <i>endo</i> / RO- <i>exo</i> : averaged	RO- <i>exo</i> / RO- <i>endo</i> : averaged
$(\mp) \text{II} \longleftrightarrow (\pm) \text{IV}$ RO- <i>endo</i> RO- <i>endo</i> ●- <i>exo</i> ●- <i>endo</i> ○- <i>exo</i> ○- <i>endo</i>	$(\mp) \text{II} \longleftrightarrow (\pm) \text{III}$ RO- <i>endo</i> RO- <i>exo</i> ●- <i>exo</i> ●- <i>exo</i> ○- <i>endo</i> ○- <i>endo</i>	$(\pm) \text{III} \longleftrightarrow (\mp) \text{IV}$ RO- <i>exo</i> RO- <i>endo</i> ●- <i>exo</i> ●- <i>endo</i> ○- <i>endo</i> ○- <i>exo</i>
●- <i>endo</i> / ●- <i>exo</i> : averaged ○- <i>exo</i> / ○- <i>endo</i> : averaged	RO- <i>endo</i> / RO- <i>exo</i> : averaged	RO- <i>exo</i> / RO- <i>endo</i> : averaged
two complete sets of signals RO- <i>exo</i> ≠ RO- <i>endo</i> ●- <i>exo/endo</i> ≠ ○- <i>exo/endo</i>	one set of signals with different <i>exo</i> and <i>endo</i> signals for symmetric D-ring (● and ○)	one set of signals with different signals for ● and ○ on the same or different side from RO

[a] The *endo* or *exo* dispositions of the substituent for the trisubstituted L-rings are indicated by RO-*endo/exo* immediately below the conformation number (I–IV) and the corresponding disposition of chemically equivalent positions (labelled ● and ○) of the symmetrical rings are indicated below. The lower row shows an indication of what would be observed in the NMR spectra: ● and ○ averaged means that chemically equivalent positions of the symmetric ring (R-ring in Scheme 6) would be observed as a single signal and RO-*endo* ≠ *exo* means that different sets of signals would be observed for the conformations with the *endo* L-ring substituent and the *exo* L-ring substituent (fast L ring rotation, left column). RO averaged means that the substituted L-ring would lead to only one set of signals but a differentiation of chemically equivalent positions of R-ring would occur (center and right columns).

served for the chemically equivalent pairs of nuclei requires a fast exchange of their positions, thus introducing more requirements into the kinematics of the system. It is interesting to note that such requirements would not have been evident if we had only analysed the previously described systems with two axially symmetric rings. In the following discussion, the possible situations accounting for the observed NMR spectra are first explored, followed by an analysis of the NMR spectra at different temperatures, and finally, the implications for the tubulin polymerisation inhibitory activities are discussed.

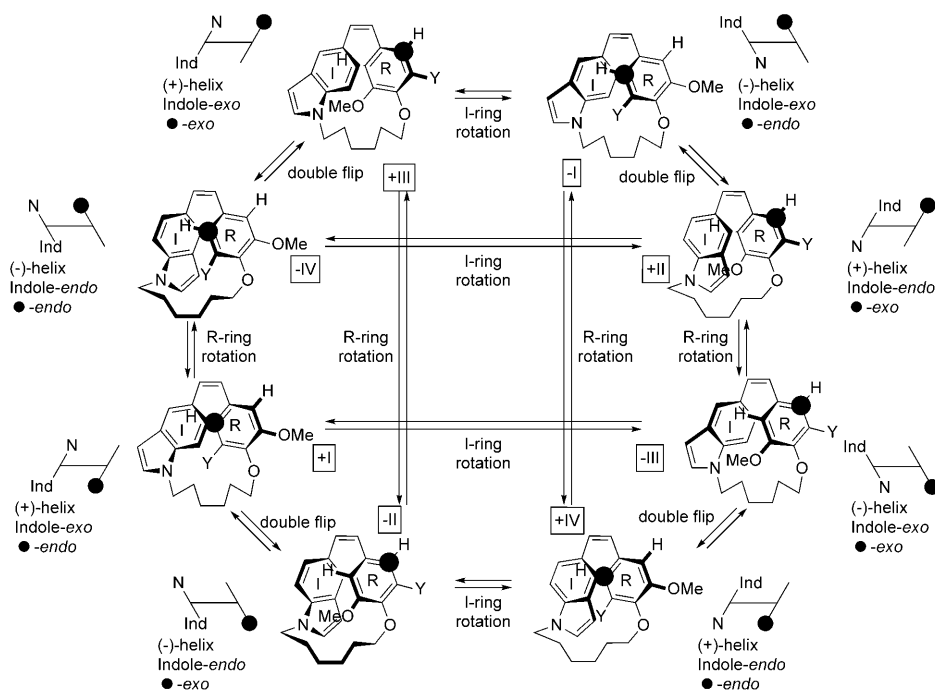
Regardless of the nature of the aromatic rings, if the three types of ring motions shown in Scheme 6 occur rapidly on the NMR timescale, an averaging of the signals for the four relevant species (I–IV) and the chemically equivalent protons (in the particular case of axially symmetric rings) would explain the simple NMR spectra observed. However, more stringent situations could also account for the observed results.

If only two of the three motions were fast on the NMR timescale, full agreement with the observed signal averaging would also be produced (Table 2) because the conformations (± I–± IV) rapidly exchange.

If only one of the three motions were fast on the NMR timescale, we should observe either two different sets of signals or two different signals for chemically equivalent pairs (Table 3 and Scheme 6). To observe a single set of signals when unsymmetrical L-ring rotation is the only fast motion, one of the equilibria should predominate over the other. For the other two cases, the only explanation for a single signal for chemically equivalent pairs of nuclei would be an accidental degeneration of the signals, arising from similar chemical environments. This explanation seems more likely for the fast double flip because when the R-ring rotation is the fast process the differences caused by the ring-current effects seem to be too important to be neglected.

Similarly, eight conformational populations can be proposed for the macrocyclic indole derivatives **17a** (Y=H) and **18a** (Y=OMe). The eight conformations have also been labelled I to IV preceded by their helical sign, as depicted in Scheme 7. Owing to the symmetry of the R-ring in compound **18a**, conformations I and III are indistinguishable, and so are II and IV, but I–IV are different in compound **17a**. The same motions depicted in Scheme 5 are responsible for the conformational transitions. The same considerations made for the appearance of the NMR spectra of **14a**, **15a** and **16a** (see above) apply to **18a**. For **17a**, with its two asymmetrically substituted rings, the predominating conformational populations must exchange rapidly on the NMR timescale to produce the observed NMR spectra.

This simplified vision of the conformational equilibria for these compounds becomes more complex if the interactions and movements of the bridge (3-oxapentamethylene and hexamethylene) are taken into account. To gain deeper insight into the conformational equilibria for **14a–18a** and the relative ease of the conformational exchanges involved in the appearance of the NMR spectra, we studied these sys-



Scheme 7. Conformational equilibria for **17a** ($Y=H$), lacking symmetric rings, and **18a** ($Y=OMe$), with one symmetric ring. Fast rotation of R- and/or I-rings through the macrocycle and/or double flip are required for the appearance of chemically equivalent positions as a single signal in NMR spectra.

tems using molecular mechanics and molecular dynamics simulations, and compared the results with those obtained for related model systems and previously described compounds.

Molecular mechanics: To establish the relevant conformations for compounds **14a–18a**, Monte Carlo conformational searches using molecular mechanics (MM3 force field with chloroform as the solvent) were carried out.^[29] The conformations found within 10 kJ mol^{-1} of the global minimum were considered relevant for the conformational equilibria studied, and automatically assigned to the conformational classes $\pm I$ to $\pm IV$, based on the dihedral angles measured between the ring planes and the double-bond plane (see the Supporting Information, pp. 7–8, for dihedral angles and conformational classes definitions). Additional categories were defined to include conformations representing states close to transitions between two classes, such as those with mismatched helical signs for the two aromatic rings, or those in which the dihedral angles of one or both ring planes with the double-bond plane are close to ($\pm 10^\circ$) the change of quadrants ($0, \pm 90, \text{ and } \pm 180^\circ$).

The most stable conformations for compounds **14a** and **15a** belong to the $\pm I/\pm III$ group, whereas for **16a** they belong to the $\pm II/\pm IV$ class. The energy differences with the alternative conformational groups are 7.3, 2.0 and 3.2 kJ mol^{-1} , respectively. For **18a**, despite the rigidity introduced into the system by the indole ring, the situation is similar to that of **14a** and **15a**, with the $\pm I/\pm III$ group pre-

dominating over the $\pm II/\pm IV$ classes, which were 7.7 kJ mol^{-1} higher in energy. For **17a**, the relative stabilities of I–IV were 1.1, 8.8, 0.0 and 1.7 kJ mol^{-1} , respectively. For all of the compounds considered, conformations close to the double flip were also frequently found. Moreover, the conformations close to ring rotations were scarcely populated. Accordingly, we considered all of the conformational groups in the discussions of the conformational equilibria (see the Supporting Information, p 9, for a summary of the conformations found for **17a** and **18a** in the Monte Carlo searches).

The X-ray crystal structure obtained for olefin **18a** (Figure 1) shows the $-I/-III$ conformation in the solid state, in good agreement with the cal-

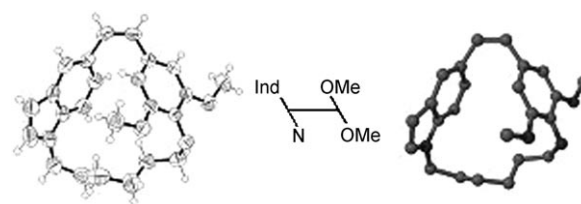


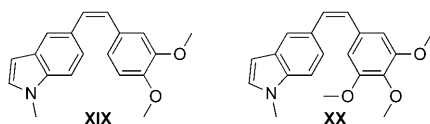
Figure 1. Structure obtained by X-ray diffraction of crystals of olefin **18a**. Ellipsoids are shown at the 30% probability level.^[38]

culations. These conformations also show dihedral angles between the planes of both rings and a double bond similar to that found in stilbene.^[26,27]

Molecular dynamics: The conformational behaviour of these macrocyclic stilbenes was investigated by means of molecular dynamics (MD) simulations at virtual temperatures of 300, 400, 600, 1000, 1200 and 1500 K, with simulation times of 3 ns (see the Supporting Information, pp. 12–17). The motions of the hexamethylene- and 3-oxapentamethylene spacers and the aromatic rings in the resulting trajectories were analysed in the same way as the results of the Monte Carlo conformational searches. When the observed conformational class changes were assignable to a single ring rotation, as depicted in Schemes 6 and 7, the transitions were labelled accordingly (e.g., if along the trajectory for **18a**, a conformation belonging to class $+III$ was followed by another belonging to $-I$, such a transition was labelled as indole-ring rotation, according to the upper row of Scheme 7). When more than one transition had to be in-

voked to explain the changes, no attempt was made to assign the motions involved.

For comparative purposes, identical simulations were carried out on **XIX** and **XX**, non-macrocyclic analogues of **17a** and **18a**, in which the hexamethylene spacers had been replaced by two methyl groups (see the Supporting Information, pp. 10–11, for the calculated simulations). The latter analogue is a very potent inhibitor of tubulin polymerisation, comparable with combretastatin A-4.^[17d] At 300 K, both non-macrocyclic analogues sample all of the conformational populations (\pm I to \pm IV); the I/III group is more populated than the II/IV group for both compounds. These preferences can be explained first in terms of the higher stability of *endo* rather than *exo*-methoxy groups (e.g., III is more stable than I for **XIX**) and, second, by a disfavoured simultaneous *endo* disposition of both the methoxy and indole (pyrrole moiety) substituents (II less favoured). At 300 K, conformations close to transitions between I and IV are also observed; the commonest ones are those corresponding to ring rotations. These conformations, stabilised by conjugation of the rotating ring with the double bond, were rarely observed for the macrocyclic analogues (see below), probably due to unfavourable contacts with the spacer. With the simulation lengths employed, it is already apparent that the compound with two methoxy groups *meta* to the olefinic bridge presents more difficulties for the rotation of the other ring (indole). As expected, simulations at higher temperatures led to more conformations apart from I to IV and to more conformational transitions. However, the relative populations of the conformational groups and transition frequencies were conserved.



The molecular dynamics simulations at 300–600 K for the macrocyclic compounds **14a–18a** are very similar to one another. For all of them, the only observed transitions were double flips. For each compound, the relative stabilities of the conformations determined their populations in the molecular dynamics trajectories. Unlike the non-macrocyclic cases described above, the preferred conformations for **14a–16a** were those with an *exo* disposition of the substituent of the trisubstituted ring, due to unfavourable interactions of the *endo* ring substituents with the spacer. The situation is also similar for indolic macrocycles **17a** and **18a**, with conformation I predominating over II. The preference for an *exo* disposition of the methoxy groups explains the greater energy difference for the two conformations found in the former than in the latter. Intermediate conformations corresponding to double flips were also frequently found along the trajectories.

As expected, simulations carried out at higher temperatures (1200 and 1500 K) revealed an increased frequency of

the conformations corresponding to transitions among conformations I–IV. However, the conformations observed for compounds **14a**, **15a**, **17a** and **18a** are the same as those at 300 K. The most remarkable difference was observed for compound **16a** at 1200 K (Figure 2). During the 3 ns simula-

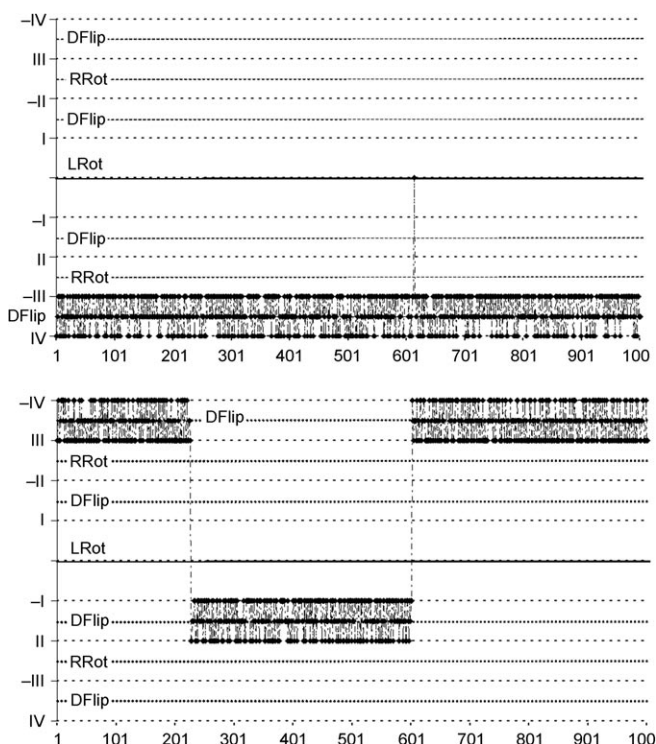


Figure 2. Conformations found along the trajectories of the molecular dynamics simulations for olefins **15a** (top) and **16a** (bottom) at 1200 K. For the latter, the trisubstituted ring rotation is evidenced by the upper to lower half crossover.

tion, double flips were often observed within the III/–IV conformational ensemble, followed by a transition from the III/–IV to the –I/II ensemble, and later by a reversal of the process. Experimental support for this result was provided by the ¹³C NMR spectra for compound **15a**, which showed two signals for each pair of equivalent carbon atoms of the disubstituted phenyl ring (Figure 3, on the left), whereas only one signal for each pair of equivalent carbon atoms of the disubstituted phenyl ring was observed for **16a** (Figure 3, on the right), according to the ease of exchange between conformational ensembles.

The situation described for the **15a** and **16a** pair is analogous to the case of related macrocyclic diols, in which ring flipping was observed for a *para*-disubstituted phenyl ring.^[12d] However, in the present case, the observed ring flip was not for the disubstituted phenyl, but for the trisubstituted one (Figure 4). This observation suggests that in these systems the interaction of the substituents on the phenyl rings with the spacer can determine the ease of rotation of the other ring. In good agreement with this observation, shortening of the spacer from a hexamethylene to a 3-oxapentamethylene hindered ring rotation for **15a**; this is re-

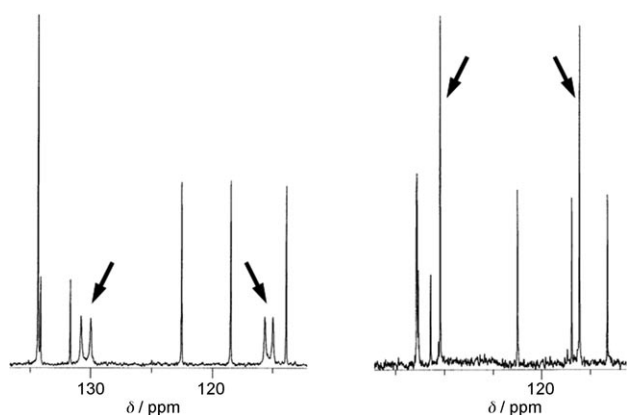


Figure 3. ^{13}C NMR (50.3 MHz) spectra for compounds **15a** (left) and **16a** (right). The chemically equivalent methines occurring as a single signal for **16a** and as two signals for **15a** are indicated by arrows.

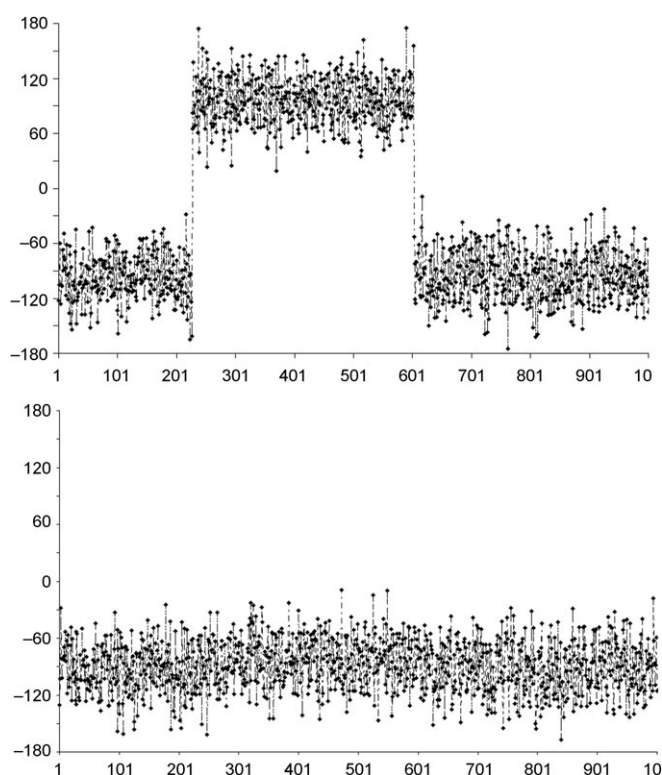


Figure 4. Dihedral values between the ring planes and the double-bond plane along the trajectories of the molecular dynamics simulations for olefin **16a** at 1200 K. The dihedral values for the trisubstituted phenyl ring are shown on the top, whereas those for the disubstituted phenyl ring are shown on the bottom, showing the rotation of the former during the molecular dynamics trajectory.

sponsible for signal differentiation for equivalent carbon atoms. The introduction of more substituents on the phenyl rings, such as in **14a**, or the more rigid indole ring of **17a** and **18a** also prevented ring rotations.

Conformational behaviour at room temperature: All of the macrocyclic olefins described herein (**14a–18a**) show NMR spectra with a single set of signals where the exchangeable

nuclei resonate isochronously, except for **15a** and **18a**, which produced broadened signals (for **15a**, duplicated signals are displayed in the ^{13}C NMR for the disubstituted symmetric ring). As discussed above, this situation can be explained if rapid interconversion between conformations I–IV occurs; rapid rotations are required for at least two of the three movements taken into account during the conformational analysis.

The observed spectra and the molecular mechanics and dynamics results are summarised in Table 4, according to the following rules:

- 1) Inspection of the molecular dynamics simulations of the macrocycles suggests that the double flip is always the fastest, whereas one ring rotations are preferred in open stilbene-like compounds (**XIX**, **XX** and reference [26b]). It also suggests how easy the other motions are (always slower than the double flip).
- 2) The larger hexamethylene spacer allows faster ring rotations (disubstituted or trisubstituted) passing hydrogen atoms through the intra-anular space. This is the case for olefin **16a**, with two fast motions (double flip and L-ring rotation).
- 3) The shorter 3-oxapentamethylene spacer reduces the intra-anular space and hinders ring rotations of passing hydrogen atoms through it. Only the double flip is fast on the NMR spectroscopy timescale and broadened signals (duplicated in the ^{13}C NMR spectra) are observed for olefin **15a**.
- 4) The rigidity introduced by the indole N–C bond slows down motions and causes the line broadening observed for the signals of the other (symmetric) ring in compound **18a**.
- 5) The appearance of only one set of signals in the case of **17a** must be explained by a slowed down motion and the predominance of one conformation (on the contrary, line broadening of two sets of signals would be observed). Conformation –I is the most populated one in the molecular dynamics.

Variable-temperature (VT) ^1H NMR spectroscopy: Although the room temperature NMR spectra for all the olefins are simple, the molecular mechanics models and the molecular dynamics simulations suggest that, at least, one-ring flips should be activated processes. VT ^1H NMR spectroscopic studies of olefins **14a–16a** in CD_3OD between 223 and 323 K in 10 K steps revealed complex kinematics. In all the cases, the observed coalescence processes are consistent with the freezing of one-ring rotations at lower temperatures.^[30] These observations agree with the MD simulations, which pinpoint this motion as the slower of the fast ones on the NMR spectroscopy timescale. The effects of this freezing are most diagnostic for the signals of the other aromatic ring.

Olefins **15a** and **16a**, differing only in the spacer (3-oxapentamethylene and hexamethylene, respectively), behaved

Table 4. Summary of ease of rotations: double flips and ring rotations for olefins **14a–18a** compared with the observed NMR spectra and explained according to molecular dynamics calculations.

	Double flip	L-ring rotation	R-ring rotation	NMR spectra	Origin	Explanation
14a	+++	+	no	one set	averaged, fast exchange	two fast motions
15a	+++	+/-	no	one set ^[a]	intermediate exchange	shorter spacer
16a	+++	+	+	one set	averaged, fast exchange	two or three fast motions
17a	+++	+/-	+/-	one set	slow exchange, one conformation predominates	rigid indole
18a	+++	+/-	no	one set ^[a]	intermediate exchange	rigid indole

[a] Signals are broadened.

in accordance with their expected different difficulty in letting the ring planes pass through the intra-annular cavity. Olefin **15a**, with the smaller cavity, already showed a substantial broadening of the signals integrating two protons of the axially symmetric ring (R ring in Scheme 6, Y=H) at room temperature. At lower temperatures, each broadened signal gave rise to two new ones that integrated to one proton each, in agreement with slower L-ring rotation. The chemical shift difference between each one of the pair of newly generated signals (ca. 0.3 ppm) could be assigned to the anisotropic field effect of the methoxy group on the opposite phenyl ring because the field effect due to the ring current should still have been averaged by the double flip. For **16a**, the larger intra-annular space gave rise to narrow, averaged signals at room temperature. A decrease in temperature resulted in substantial line broadening of the signals of the axially symmetric ring, which were no longer observed below 233 K. Similar behaviour was observed for **14a**.

Olefin **18a** followed the guidelines indicated for **15a**, with a similar temperature dependency. The aromatic and methoxy protons of the dimethoxy-substituted phenyl ring were broadened and signal averaged at room temperature and they were not observable at 273 K. They reappeared and progressively sharpened up as two new pairs of signals from 263 down to 213 K. In this case, the chemical shift dispersion of about 1 ppm between the chemically equivalent proton pairs could be assigned to the anisotropic field effect of the indole ring, whose frozen rotation reveals the predominance of the *endo* (I and III) versus *exo* (II and IV) conformations, connected by fast double flips.

Olefin **17a** does not have an axially symmetric ring, which precludes the observation of mutual exchange behaviour as described above. On the contrary, it shows a non-mutual exchange, resulting from the freezing of the same processes as before. The observed temperature dependency is in between that of **15a** and that of **16a**. Signal averaging was observed at room temperature and a single residual conformer was seen, the signals of which became substantially line broadened between 273 and 253 K. They were unobservable down to 233 K and reappeared as two new pairs of broadened signals at 213 K, which corresponded to two different residual

conformers in a ratio of about 7:3 ratio. The most affected signals were those corresponding to the aromatic protons and the methoxy group of the monomethoxylated phenyl ring. Again, the magnitude of the chemical shift differences for the residual conformers could be assigned to the anisotropic field effect of the indole ring. In the minor conformer (belonging to conformation-type III in Scheme 7, Y=H), the methoxy group and its *ortho* proton were upfield shifted with respect to those of

the major conformer, which corresponded to conformation I in Scheme 7. The large chemical shift difference suggested a minor, if any, contribution of conformations II and IV to the overall equilibrium. These results are in full agreement with the results of the molecular mechanics for **17a** and the non-macrocyclic analogue **XIX**, previously discussed.

Tubulin polymerisation inhibition: These macrocyclic stilbenes are the first of their class to show tubulin polymerisation inhibition (TPI) (Table 5).^[31] Comparison of the ac-

Table 5. Tubulin polymerisation inhibitory activity of the macrocyclic olefins **14a–18a**.^[a]

Compound	TPI [%] (c [μM])
XXI ^[12c]	60 (40)
14a	0 (40)
15a	44 (20)
16a	48 (20)
17a	19 (20)
18a	44 (20)

[a] **XXI**=stilbenophane (Z=CH₂-CH₂) in Scheme 1.

cessible conformations for the macrocyclic ligands **14a–18a** with the X-ray crystal structures of podophyllotoxin and DAMA-colchicine complexed with tubulin^[32] revealed that the relevant ones are +I and/or +III (Figure 5). The TPI assays were carried out at 37°C with incubation times of minutes or more. By taking into account the dynamic behaviour shown by the olefins, conformational equilibration should not then be an issue. Therefore, the similar conformations adopted by **15a** and **16a** lead to similar TPI potencies, despite their different dynamic behaviour. Furthermore, for all of the studied olefins, conformational classes I/III are the more stable ones. Accordingly, the observed differences in potency should be explained by considering the structures of the favoured conformations.

The great structural similarity observed among the macrocyclic stilbenes indicates differences in the substituents to explain the differences in potency. First of all, the similar behaviour of **15a**, **16a** and **XXI**, the olefin with one more me-

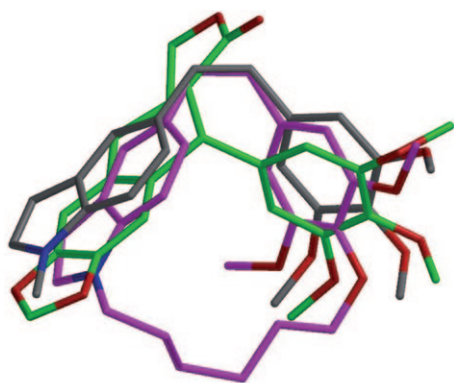


Figure 5. Superposition of podophyllotoxin (carbon atoms shown in green), **XX** (carbon atoms shown in grey) and **18a** (carbon atoms shown in pink). The structure of podophyllotoxin was obtained by X-ray crystal structure analysis.^[32] The structures of **XX** and **18a** were generated by docking with Autodock 4.0, following a described procedure.^[17e] Compounds **18a** and **XX** belong to the conformational class +I/+III.

thoxy group (the macrocyclic equivalent of deoxyCA-4), should not pass unnoticed. This is the first case of the replacement of the trimethoxyphenyl ring of combretastatin analogues (the central methoxy group of the dimethoxylated ring of the macrocyclic olefins is represented by the spacer) by a moiety with one less methoxy group without severe reductions in potency. This observation suggests a favourable replacement of such a moiety by the spacer, as we had previously anticipated.^[12c]

On the other hand, for the indolic analogues, the macrocycle with a single methoxy group (**17a**) is less potent than the dimethoxylated counterpart (**18a**). The rigidity of the indole forces the spacer of the +I/III conformations of the indolic olefins towards the opposite side of the methoxy group that lies under the phenyl ring of the indole in the complex with tubulin (Figure 5). In the more flexible phenylic olefins it can go more along the double-bond plane, thus replacing the aforementioned methoxy group. This suggestion is supported by the X-ray crystal structure of E7030 complexed with tubulin, which shows that the inner methoxy group can be replaced by a hydrogen atom in pyridine-based colchicine site ligands.^[33] This observation is important for the establishment of consistent structure–activity relationships for colchicine site ligands because the trimethoxyphenyl ring has often been seen as a requirement in some families of analogues and is absent in other families.

The lack of activity observed for **14a**, which had higher structural resemblance to combretastatin A-4 than **15a** and **16a**, could also be explained by a preferential binding of conformational classes +I and/or +III. If the spacer, as stated above for the indolic macrocycles, fills the concave side of the molecule, the hydroxyl group must point towards the convex side of the molecule. The lack of activity observed for **14a**, thus arises again from the departure of the spacer from the plane of double bond, as previously indicated for indoles.

These compounds were tested against HeLa, HT-29, A-549 and HL-60 cell lines, but they were not cytotoxic at the concentrations of $\leq 1 \mu\text{M}$ assayed (higher concentrations were not used owing to solubility problems).

Conclusion

The synthesis of new stilbenophanes has been accomplished by using the McMurry methodology to produce analogues of antimittotic combretastatins. The presence of a bridge between *para-para* positions modifies the dynamics of these molecules in comparison with those of non-macrocyclic stilbene analogues. Conformational analysis of these compounds was carried out by taking into account ring flips, ring rotations and the effect of the bridge; these results were in agreement with the molecular calculations and NMR spectra. These macrocyclic analogues are the first of their class to inhibit tubulin polymerisation, giving a further insight into the structural requirements of the colchicine site of tubulin. The activity results for these macrocycles have been rationalised in terms of mobility and steric hindrance.

Experimental Section

General: Reagents were used as purchased without further purification. Solvents (THF, DMF, CH_2Cl_2 , and toluene) were dried and freshly distilled before use according to procedures described in the literature. Chromatographic separations were performed on silica-gel columns by flash (Kieselgel 40, 0.040–0.063; Merck) or gravity (Kieselgel 60, 0.063–0.200 mm; Merck) chromatography. TLC was performed on precoated silica-gel polyester plates (0.25 mm thickness) with a UV fluorescence indicator 254 (Polychrom SI F₂₅₄). Melting points were determined on a Buchi 510 apparatus and are uncorrected. ^1H and ^{13}C NMR spectra were recorded in CDCl_3 at 25 °C on a Bruker WP 200-SY spectrometer at 200/50 MHz or on a Bruker SY spectrometer at 400/100 MHz. Chemical shifts (δ) are given in ppm downfield from tetramethylsilane as the internal standard and coupling constants (J values) are in hertz. IR spectra were run on a Nicolet Impact 410 spectrophotometer. GC-MS analyses were carried out with a Hewlett–Packard 5890 Series II apparatus (70 eV). For FAB HRMS analyses, a VG-TS250 apparatus (70 eV) was used. HPLC separations were run on at least three different columns (5 mm, 4.6×150 mm): Waters X-Terra MS C₈, Waters X-Terra MS C₁₈ and Waters X-Terra MS C_F on an Agilent HP series 1100 with at least two different solvent gradients (typically acetonitrile/water or methanol/water). Elemental analyses were run on a Perkin–Elmer 2400 CHN apparatus.

Compounds **1–3** were obtained as previously described,^[12] whereas intermediates **4–11** were produced by the Mitsunobu method, phase transfer or direct alkylations, by following the procedures described below.

General procedure for the Mitsunobu reactions producing dialdehydes 4–6: A mixture of the hydroxy aldehyde (**1–3**), the PPh₃ resin (0.76–1.01 mol/mol of aldehyde, except for the synthesis of **4**, 2.32 mol/mol of **1**), and the phenolic aldehyde (0.96–1.50 mol/mol of aldehyde, except for the synthesis of **4**, because a large excess of 3.42 mol of 3,4-dihydroxybenzaldehyde/mol of **1** was used to avoid dialkylations) in dry CH_2Cl_2 (8–19 mL/mmol of aldehyde) was stirred for 1–3 h before the slow addition of DBAD or DIAD (0.76–1.01 mol/mol of aldehyde; in the synthesis of **4**, 2.31 mol of DBAD/mol of **1** were used) at RT. After 48 h the reactions were filtered and the resin was washed with EtOAc. The combined organic layers were evaporated, dissolved in EtOAc and washed with

NaOH (4%) and brine until the pH of the solution was neutral. Once dried and evaporated, the crude reaction products were purified by flash chromatography (hexane/EtOAc mixtures).

Compound 4: ¹H NMR (400 MHz): δ = 3.86–3.88 (m, 2H; CH₂), 3.91 (s, 6H; 2 × CH₃), 3.97–3.99 (m, 2H; CH₂), 4.30–4.32 (m, 4H; 2 × CH₂), 6.99 (d, *J* = 7.9 Hz, 1H; Ar-H), 7.37 (d, *J* = 1.8 Hz, 1H; Ar-H), 7.41–7.43 (m, 1H; Ar-H), 7.42 (s, 2H; Ar-H), 9.84 (s, 1H; CHO), 9.86 ppm (s, 1H; CHO); ¹³C NMR (100.6 MHz): δ = 56.5 (2 × CH₃), 69.5 (2 × CH₂), 71.0 (CH₂), 72.6 (CH₂), 107.0 (CH), 113.3 (CH), 115.3 (CH), 124.2 (CH), 131.3 (C), 132.2 (C), 142.7 (C), 147.5 (C), 151.6 (C), 154.0 (2 × C), 191.4 (CH), 191.4 ppm (CH); FTIR: $\tilde{\nu}$ = 3341, 1689, 1607, 1507, 1127 cm⁻¹.

Compound 5: ¹H NMR (400 MHz): δ = 1.59–1.61 (m, 4H; 2 × CH₂), 1.79–1.81 (m, 4H; 2 × CH₂), 3.91 (s, 6H; 2 × CH₃), 3.99–4.01 (m, 2H; CH₂), 4.09–4.10 (m, 2H; CH₂), 6.95 (d, *J* = 8.3 Hz, 1H; Ar-H), 7.12 (s, 2H; 2 × CH), 7.40 (d, *J* = 8.3 Hz, 1H; Ar-H), 7.43 (brs, 1H; Ar-H), 9.82 (s, 1H; CHO), 9.86 ppm (s, 1H; CHO); ¹³C NMR (100.6 MHz): δ = 25.5 (2 × CH₃), 28.8 (CH₂), 30.0 (CH₂), 56.1 (2 × CH₃), 69.5 (CH₂), 73.2 (CH₂), 106.7 (2 × CH), 111.1 (CH), 114.0 (CH), 124.6 (CH), 130.1 (C), 131.5 (C), 142.8 (C), 142.8 (C), 151.9 (2 × C), 153.3 (C), 171.2 (C), 191.1 (CH), 191.1 ppm (CH); FTIR: $\tilde{\nu}$ = 3309, 2276, 1688, 1508, 1127 cm⁻¹.

Compound 6: ¹H NMR (400 MHz): δ = 3.65 (s, 3H; CH₃), 3.73–3.77 (m, 4H; 2 × CH₂), 3.98–4.06 (m, 4H; 2 × CH₂), 6.78 (d, *J* = 8.8 Hz, 2H; 2 × CH), 7.16–7.20 (m, 3H; Ar-H), 7.59 (d, *J* = 8.8 Hz, 2H; 2 × CH), 9.61 (s, 1H; CHO), 9.64 ppm (s, 1H; CHO); ¹³C NMR (100.6 MHz): δ = 55.7 (CH₃), 67.7 (CH₂), 68.4 (CH₂), 69.5 (2 × CH₂), 109.3 (CH), 111.8 (CH), 114.8 (2 × CH), 126.4 (CH), 129.9 (C), 130.1 (C), 131.8 (2 × CH), 149.7 (C), 153.7 (C), 163.7 (C), 190.7 (CH), 190.9 ppm (CH); FTIR: $\tilde{\nu}$ = 1683, 1595, 1511, 1268, 1132 cm⁻¹.

Phase-transfer synthesis of 7: Vanillin (5.52 g, 36.3 mmol), NaOH (2.27 g, 56.8 mmol), 1,6-dibromohexane (12.0 mL, 19.0 g, 78.0 mmol) and tetrabutylammonium bromide (1.90 g, 5.89 mmol) were added to a heterogeneous mixture of CH₂Cl₂ (190 mL) and water (190 mL). The reaction was stirred for 48 h., separated and the aqueous layer extracted with CH₂Cl₂. The combined organic layers were successively washed with NaOH (4%) and brine, dried (Na₂SO₄) and evaporated. After column chromatography (SiO₂) with hexanes and CH₂Cl₂, bromoaldehyde **7** (8.13 g, 25.8 mmol, 71%) was obtained as a brown solid, which was crystallised in CH₂Cl₂/hexane. M.p. 45°C; ¹H NMR (400 MHz): δ = 1.55–1.57 (m, 4H; 2 × CH₂), 1.86–1.93 (m, 4H; 2 × CH₂), 3.40 (t, *J* = 6.6 Hz, 2H; CH₂), 3.89 (s, 3H; CH₃), 4.08 (t, *J* = 6.6 Hz, 2H; CH₂), 6.94 (d, *J* = 8.0 Hz, 1H; Ar-H), 7.38 (d, *J* = 1.8 Hz, 1H; Ar-H), 7.41 (dd, *J* = 1.8, 8.0 Hz, 1H; Ar-H), 9.81 ppm (s, 1H; CHO); ¹³C NMR (100.6 MHz): δ = 25.1 (CH₃), 27.8 (CH₂), 28.7 (CH₂), 32.6 (CH₂), 33.8 (CH₂), 55.9 (CH₃), 68.8 (CH₂), 109.2 (CH), 111.4 (CH), 126.6 (CH), 129.8 (C), 149.7 (C), 154.0 (C), 190.7 ppm (CHO); FTIR: $\tilde{\nu}$ = 1684, 1589, 1511, 1269, 1134 cm⁻¹; MS: *m/z* (%): 314 (4), 316 (4) [*M*⁺], 152 (100).

Direct alkylation synthesis of 8: A solution of *p*-hydroxybenzaldehyde (1.22 g, 10.0 mmol), K₂CO₃ (4.84 g, 35.0 mmol) and bromoaldehyde **7** (2.07 g, 6.57 mmol) in dry DMF (30 mL) was maintained for 48 h at 60°C under argon. The solvent was evaporated in vacuo and the crude reaction mixture was extracted with CH₂Cl₂ and 2N HCl, and the organic layer was washed with brine and dried. By column chromatography (SiO₂) using CH₂Cl₂/AcOEt (10:1) and 1% of triethylamine (TEA), dialdehyde **8** (1.08 g, 3.03 mmol; 46%) was obtained as a white solid, which was recrystallised in CH₂Cl₂/hexane. M.p. 78°C; ¹H NMR (400 MHz): δ = 1.48–1.51 (m, 4H; 2 × CH₂), 1.77–1.80 (m, 4H; 2 × CH₂), 3.86 (s, 3H; CH₃), 3.96–4.07 (m, 4H; 2 × CH₂), 6.92 (d, *J* = 8.0 Hz, 1H; Ar-H), 6.93 (d, *J* = 8.8 Hz, 2H; 2 × Ar-H), 7.35 (d, *J* = 1.8 Hz, 1H; Ar-H), 7.38 (dd, *J* = 1.8, 8.0 Hz, 1H; Ar-H), 7.76 (d, *J* = 8.8 Hz, 2H; 2 × Ar-H), 9.78 (s, 1H; CHO), 9.81 ppm (s, 1H; CHO); ¹³C NMR (100.6 MHz): δ = 25.8 (2 × CH₃), 28.9 (2 × CH₂), 56.0 (CH₃), 68.2 (CH₂), 68.9 (CH₂), 109.3 (CH), 111.4 (CH), 114.8 (2 × CH), 126.8 (CH), 129.8 (C), 130.0 (C), 132.0 (2 × CH), 149.8 (C), 154.1 (C), 161.2 (C), 190.8 (CHO), 190.9 ppm (CHO); FTIR: $\tilde{\nu}$ = 1683, 1596, 1511, 1267, 1160, 1135, 1012 cm⁻¹; MS: *m/z* (%): 356 (65) [*M*⁺], 152 (100).

Phase-transfer synthesis of 9: By following the procedure described above, 1*H*-indole-5-carbaldehyde (2.00 g, 13.80 mmol), NaOH (1.10 g, 27.60 mmol) and tetrabutylammonium hydrogen sulfate (200 mg,

0.59 mmol) in CH₂Cl₂ (40 mL) were stirred for 1 h, after which 1,6-dibromohexane (4.25 mL, 6.74 g, 27.60 mmol) was added and the mixture was maintained for 48 h at RT. The crude product was extracted from a SiO₂ column with hexane and CH₂Cl₂ to yield bromoaldehyde **9** (3.04 g, 9.90 mmol, 71.7%). ¹H NMR (200 MHz): δ = 1.28–1.32 (m, 2H; CH₂), 1.36–1.38 (m, 2H; CH₂), 1.76–1.78 (m, 2H; CH₂), 1.80–1.82 (m, 2H; CH₂), 3.32 (t, *J* = 6.6 Hz, 2H; CH₂), 4.09 (t, *J* = 7.0 Hz, 2H; CH₂), 6.62 (d, *J* = 3.3 Hz, 1H; Ar-H); 7.15 (d, *J* = 3.3 Hz, 1H; Ar-H), 7.37 (d, *J* = 8.4 Hz, 1H; Ar-H), 7.74 (dd, *J* = 8.4, 1.5 Hz, 1H; Ar-H), 8.10 (d, *J* = 1.5 Hz, 1H; Ar-H), 9.99 ppm (s, 1H; CHO); ¹³C NMR (50.3 MHz): δ = 26.1 (CH₂), 27.7 (CH₂), 30.1 (CH₂), 32.6 (CH₂), 33.8 (CH₂), 46.5 (CH₂), 103.4 (CH), 110.0 (CH), 121.7 (CH), 126.5 (CH), 128.4 (C), 129.3 (C), 129.9 (CH), 139.3 (C), 192.4 ppm (CH).

Direct alkylation synthesis of 10: A solution of vanillin (1.72 g, 11.30 mmol) and K₂CO₃ (10.00 g, 7.25 mmol) in dry DMF (40 mL) was stirred for 0.5 h. Then, bromoaldehyde **9** (2.90 g, 9.44 mmol) in DMF (10 mL) was added and the reaction was maintained for 48 h at 70°C under argon. The mixture was poured into hexane (150 mL), filtered, and the solvent was evaporated in vacuo. The crude reaction mixture was re-dissolved in CH₂Cl₂, washed with NaOH (4%) and brine, and evaporated to yield dialdehyde **10** (3.41 g, 9.34 mmol; 98%). ¹H NMR (400 MHz): δ = 1.35–1.43 (m, 2H; CH₂), 1.45–1.47 (m, 2H; CH₂), 1.82–1.84 (m, 2H; CH₂), 1.85–1.87 (m, 2H; CH₂), 3.89 (s, 3H; CH₃), 4.05 (t, *J* = 6.6 Hz, 2H; CH₂), 4.17 (t, *J* = 7.0 Hz, 2H; CH₂), 6.62 (d, *J* = 3.3 Hz, 1H; Ar-H), 6.91 (d, *J* = 8.4 Hz, 1H; Ar-H), 7.18 (d, *J* = 3.3 Hz, 1H; Ar-H), 7.39–7.43 (m, 3H; Ar-H), 7.70 (dd, *J* = 8.4, 1.4 Hz, 1H; Ar-H), 8.13 (d, *J* = 1.4, 1H; Ar-H), 9.83 (s, 1H; CHO), 10.00 ppm (s, 1H; CHO); ¹³C NMR (100.6 MHz): δ = 25.4 (CH₃), 26.4 (CH₂), 28.7 (CH₂), 30.0 (CH₂), 46.3 (CH₂), 55.8 (CH₃), 68.7 (CH₂), 103.2 (CH), 109.3 (CH), 110.0 (CH), 111.4 (CH), 121.5 (CH), 126.4 (CH), 126.6 (CH), 128.3 (C), 129.2 (C), 129.8 (CH), 129.8 (C), 139.2 (C), 149.7 (C), 154.0 (C), 190.7 (CH), 192.2 ppm (CH); FTIR: $\tilde{\nu}$ = 1693, 1596, 808, cm⁻¹.

Direct alkylation synthesis of 11: A solution of syringaldehyde (2.16 g, 11.87 mmol) and K₂CO₃ (10.00 g, 7.25 mmol) in dry DMF (40 mL) was stirred for 0.5 h. Then, bromoaldehyde **9** (3.05 g, 9.89 mmol) in DMF (10 mL) was added and the mixture was maintained for 48 h at 70°C under argon. The mixture was poured into hexane (150 mL), filtered and the solvent was evaporated in vacuo. The crude reaction mixture was re-dissolved in CH₂Cl₂, washed with NaOH (4%) and brine, and evaporated to yield dialdehyde **11** (3.30 g, 8.35 mmol; 85%). ¹H NMR (400 MHz): δ = 1.20–1.22 (m, 2H; CH₂), 1.40–1.43 (m, 2H; CH₂), 1.64–1.67 (m, 2H; CH₂), 1.71–1.74 (m, 2H; CH₂), 3.71 (s, 6H; 2 × CH₃), 3.91–3.95 (m, 2H; CH₂), 3.98–4.01 (m, 2H; CH₂), 6.48 (d, *J* = 3.3 Hz, 1H; Ar-H), 6.97 (s, 2H; 2 × Ar-H), 7.07 (d, *J* = 3.3 Hz, 1H; Ar-H), 7.26 (d, *J* = 8.4 Hz, 1H; Ar-H), 7.61 (d, *J* = 8.4 Hz, 1H; Ar-H), 7.96 (s, 1H; Ar-H), 9.70 (s, 1H; CHO), 9.85 ppm (s, 1H; CHO); ¹³C NMR (100.6 MHz): δ = 25.4 (CH₂), 26.5 (CH₂), 29.9 (CH₂), 30.2 (CH₂), 46.5 (CH₂), 56.1 (2 × CH₃), 73.2 (CH₂), 103.2 (CH), 106.6 (2 × CH), 110.0 (CH), 121.4 (CH), 126.4 (CH), 128.2 (C), 129.1 (C), 129.9 (CH), 131.6 (C), 139.2 (C), 142.7 (C), 153.8 (2 × C), 191.1 (CH), 192.3 ppm (CH).

General procedure for McMurry reactions: Mixtures of TiCl₄ 98% (5–10 mol/mol of dialdehyde) and Zn (10–20 mol/mol of dialdehyde) in dry THF (20–100 mL/mol of dialdehyde) were prepared at 0°C and heated at reflux for 30 min. Then, solutions of dialdehydes (**4**, **5**, **6**, **8**, **10** or **11**) in dry THF (20–40 mL/mol of dialdehyde) were added and maintained at either room temperature or under reflux conditions. The reactions were poured into mixtures of EtOAc and 2M HCl; the aqueous layer was extracted and the combined organic layers were worked up. Olefins were separated by chromatography (SiO₂, hexane/EtOAc mixtures with 0.1% triethylamine). For details about temperature, time, crude product and isolated yields, see Table 1.

Reaction of dialdehyde 4 (Table 1, entry 1): By treatment of dialdehyde **4** (260 mg, 0.6 mmol) with a mixture of Zn (430 mg, 6.6 mmol) and TiCl₄ (0.4 mL, 3.5 mmol) in THF (25 mL) under reflux for 5 h, the crude reaction product (245 mg) was obtained after the described workup. Olefin **13a** was not detected in the crude reaction mixture, which contained a mixture of diols **13b** and **13c**.

Reaction of dialdehyde 5: Synthesis of olefin 14a (Table 1, entry 2): By treatment of dialdehyde **5** (800 mg, 2.0 mmol) with a mixture of Zn (1300 mg, 20.0 mmol) and TiCl_4 (1.1 mL, 9.7 mmol) in THF (130 mL) under reflux for 24 h, the crude reaction product (785 mg) was obtained after the described workup. Chromatographic separation afforded **14a** (290 mg, 0.80 mmol, 40%). $^1\text{H NMR}$ (400 MHz): δ = 1.1–1.6 (m, 8H; 4 \times CH_2), 3.65 (s, 6H; 2 \times CH_3), 4.11–4.08 (m, 4H; 2 \times CH_2), 6.13 (s, 2H; 2 \times Ar-H), 6.20 (dd, J = 1.9, 8.4 Hz, 1H; Ar-H), 6.51 (d, J = 8.4 Hz, 1H; Ar-H), 6.70 (d, J = 1.9 Hz, 1H; Ar-H), 6.88 ppm (brs, 2H; 2 \times Olef-H); $^{13}\text{C NMR}$ (100.6 MHz): δ = 26.5 (CH_2), 27.0 (CH_2), 29.6 (CH_2), 30.0 (CH_2), 55.8 (2 \times CH_3), 69.8 (CH_2), 71.6 (CH_2), 106.8 (2 \times CH), 114.3 (CH), 115.4 (CH), 121.8 (CH), 133.1 (C), 133.3 (CH), 133.7 (CH), 134.0 (C), 132.8 (C), 142.1 (C), 142.5 (C), 152.6 ppm (2 \times C); FTIR: $\tilde{\nu}$ = 3420, 1580, 1503, 1123 cm^{-1} .

Reaction of dialdehyde 5 (Table 1, entry 3): By treatment of dialdehyde **5** (315 mg, 0.8 mmol) with a mixture of Zn (523 mg, 8.0 mmol) and TiCl_4 (0.5 mL, 4.4 mmol) in THF (25 mL) at 0°C for 5 h, the crude reaction product (370 mg) was obtained after the described workup. Olefin **14a** was not detected in the crude reaction mixture and the mixture (**14b/14c** 1/3) could not be separated by chromatography.

Reaction of dialdehyde 6: Synthesis of olefin 15a (Table 1, entry 4). By treatment of dialdehyde **6** (640 mg, 1.86 mmol) with a mixture of Zn (3820 mg, 58.4 mmol) and TiCl_4 (2.0 mL, 18.2 mmol) in THF (300 mL) at reflux for 24 h, the crude reaction product (580 mg) was obtained after the described workup. Chromatographic separation afforded **15a** (87 mg, 0.28 mmol, 15%) and diols **15b** and **15c**. **15a**: $^1\text{H NMR}$ (400 MHz): δ = 3.55–3.58 (m, 4H; 2 \times CH_2), 3.66 (s, 3H; CH_3), 4.23–4.26 (m, 4H; 2 \times CH_2), 6.26 (dd, J = 8.5, 1.8 Hz, 1H; Ar-H), 6.27 (d, J = 1.8 Hz, 1H; Ar-H), 6.5–6.7 (m, 4H; Ar-H), 6.69 (d, J = 8.5 Hz, 1H; Ar-H), 6.97 (d, J = 10.0 Hz, 1H; Olef-H), 7.00 ppm (d, J = 10.0, 1H; Olef-H); $^{13}\text{C NMR}$ (100.6 MHz): δ = 55.5 (CH_3), 68.0 (CH_2), 72.0 (CH_2), 72.4 (CH_2), 72.5 (CH_2), 113.9 (CH), 115.0 (CH), 115.7 (CH), 118.5 (CH), 122.6 (CH), 130.0 (CH), 130.8 (CH), 131.7 (C), 134.2 (C), 134.4 (2 \times CH), 146.9 (C), 150.3 (C), 157.1 ppm (C); FTIR: $\tilde{\nu}$ = 1609, 1505, 1262, 1228, 1118 cm^{-1} .

Reaction of dialdehyde 8: Synthesis of olefin 16a (Table 1, entry 5): By treatment of dialdehyde **8** (850 mg, 2.39 mmol) with a mixture of Zn (4600 mg, 70.3 mmol) and TiCl_4 (2.7 mL, 24.6 mmol) in THF (300 mL) under reflux for 24 h, the crude reaction product (670 mg) was obtained after the described workup. Chromatographic separation afforded **16a** (52 mg, 0.16 mmol, 7%). $^1\text{H NMR}$ (400 MHz): δ = 1.29–1.21 (m, 4H; 2 \times CH_2), 1.46–1.39 (m, 4H; 2 \times CH_2), 3.71 (s, 3H; CH_3), 4.05 (t, J = 7.8 Hz, 2H; CH_2), 4.11 (t, J = 7.5 Hz, 2H; CH_2), 6.25 (dd, J = 8.2, 1.9 Hz, 1H; Ar-H), 6.52 (d, J = 1.9 Hz, 1H; Ar-H), 6.56 (d, J = 8.2 Hz, 1H; Ar-H), 6.62 (d, J = 8.6 Hz, 2H; 2 \times Ar-H), 6.77 (d, J = 8.6 Hz, 2H; 2 \times Ar-H), 6.84 (d, J = 10.8 Hz, 1H; Olef-H), 6.87 ppm (d, J = 10.8 Hz, 1H; Olef-H); $^{13}\text{C NMR}$ (100.6 MHz): δ = 23.6 (2 \times CH_2), 25.6 (CH_2), 26.0 (CH_2), 55.6 (CH_3), 68.1 (CH_2), 69.7 (CH_2), 113.3 (CH), 116.1 (2 \times CH), 116.9 (CH), 122.5 (CH), 130.4 (2 \times CH), 131.4 (C), 132.7 (C), 132.8 (2 \times CH), 144.5 (C), 150.3 (C), 155.9 ppm (C); FTIR: $\tilde{\nu}$ = 1601, 1505, 1257, 1233, 1131 cm^{-1} .

Reaction of dialdehyde 8 (Table 1, entry 6): By treatment of dialdehyde **8** (62 mg, 0.17 mmol) with a mixture of Zn (343 mg, 5.25 mmol) and TiCl_4 (0.20 mL, 1.77 mmol) in THF (100 mL) at room temperature for 24 h, the crude reaction product (57 mg; 35/65 mixture of **16b** + **16c**) was obtained after the described workup.

Reaction of dialdehyde 10: Synthesis of olefin 17a (Table 1, entries 7 and 8): By treatment of dialdehyde **10** (1660 mg, 4.54 mmol) with a mixture of Zn (6430 mg, 96.8 mmol) and TiCl_4 (5.3 mL, 47.1 mmol) in THF (300 mL) at reflux for 5 h, the crude reaction product (1610 mg) was obtained after the described workup. Chromatographic separation afforded **17a** (158 mg, 0.46 mmol, 10.1%) and diols **17b** and **17c**. **17a**: $^1\text{H NMR}$ (400 MHz): δ = 0.92–0.95 (m, 2H; CH_2), 1.17–1.19 (m, 2H; CH_2), 1.32–1.35 (m, 2H; CH_2), 1.61–1.64 (m, 2H; CH_2), 3.55 (s, 3H; CH_3), 3.98 (t, J = 7.7 Hz, 2H; CH_2), 4.05 (t, J = 6.2 Hz, 2H; CH_2), 6.25 (dd, J = 8.1, 1.8 Hz, 1H; Ar-H), 6.38 (dd, J = 7.9, 1.8 Hz, 1H; Ar-H), 6.40 (d, J = 2.7 Hz, 1H; Ar-H), 6.44 (brs, 1H; Ar-H), 6.47 (d, J = 8.1 Hz, 1H; Ar-H), 6.83 (d, J = 7.9 Hz, 1H; Ar-H), 6.92 (d, J = 10.2 Hz, 1H; Olef-H), 6.96 (d,

J = 2.7 Hz, 1H; Ar-H) 7.14 (d, J = 10.2 Hz, 1H; Olef-H), 7.40 ppm (s, 1H; Ar-H); $^{13}\text{C NMR}$ (100.6 MHz): δ = 23.2 (CH_2), 25.9 (CH_2), 27.2 (CH_2), 29.5 (CH_2), 46.1 (CH_2), 55.4 (CH_3), 70.3 (CH_2), 101.0 (CH), 109.2 (CH), 113.9 (CH), 117.9 (CH), 120.5 (CH), 122.5 (CH), 124.6 (CH), 128.2 (C), 128.2 (CH), 129.8 (C), 132.9 (CH), 133.6 (C), 134.8 (CH), 135.0 (C), 144.9 (C), 150.3 ppm (C); FTIR: $\tilde{\nu}$ = 1509, 1262 cm^{-1} .

Reaction of dialdehyde 11: Synthesis of olefin 18a (Table 1, entry 9): By treatment of dialdehyde **11** (570 mg, 1.44 mmol) with a mixture of Zn (2040 mg, 30.7 mmol) and TiCl_4 (1.8 mL, 16.3 mmol) in THF (300 mL) under reflux for 5 h, the crude reaction product (680 mg) was obtained after the described workup. Chromatographic separation afforded **18a** (150 mg, 0.43 mmol, 26.7%) and diols **18b** and **18c**. **18a**: $^1\text{H NMR}$ (400 MHz): δ = 0.90–0.94 (m, 2H; CH_2), 1.23–1.26 (m, 4H; 2 \times CH_2), 1.61–1.64 (m, 2H; CH_2), 3.45 (brs, 6H; 2 \times CH_3), 3.98 (t, J = 6.4 Hz, 2H; CH_2), 4.06 (t, J = 5.9 Hz, 2H; CH_2), 6.05 (brs, 2H; 2 \times Ar-H), 6.39 (d, J = 3.1 Hz, 1H; Ar-H), 6.45 (dd, J = 8.2, 1.4 Hz, 1H; Ar-H), 6.87 (d, J = 8.2 Hz, 1H; Ar-H), 6.92 (d, J = 10.1 Hz, 1H; Olef-H), 6.97 (d, J = 3.1 Hz, 1H; Ar-H), 7.16 (d, J = 10.1 Hz, 1H; Olef-H), 7.40 ppm (s, 1H; Ar-H); $^{13}\text{C NMR}$ (100.6 MHz): δ = 23.4 (CH_2), 26.0 (CH_2), 27.8 (CH_2), 29.9 (CH_2), 45.7 (CH_2), 55.6 (2 \times CH_3), 71.8 (CH_2), 101.0 (CH), 107.2 (2 \times CH), 109.3 (CH), 120.4 (CH), 124.2 (CH), 128.0 (C), 128.1 (CH), 129.8 (C), 133.4 (CH), 133.9 (C), 134.5 (C), 134.9 (CH), 135.1 (C), 152.4 ppm (2 \times C); FTIR: $\tilde{\nu}$ = 1577, 1126 cm^{-1} .

Tubulin isolation: Calf brain microtubule protein (MTP) was purified by two cycles of temperature-dependent assembly/disassembly, according to the method of Shelanski et al.^[34] modified as described in the literature.^[35] The solution of MTP was stored at -80°C . Protein concentrations were determined by the method of Bradford^[36] by using bovine serum albumin (BSA) as standard. Four different MTP preparations were used in the tubulin assembly assays.

Tubulin assembly: In vitro tubulin self-assembly was monitored turbidimetrically at 450 nm by using a thermostated Thermospectronic Helios α spectrophotometer fitted with a Peltier temperature controller and a circulating water carousel system. The ligands were dissolved in DMSO and stored at -20°C . The amount of DMSO in the assays was 4%, which has been reported not to interfere with the assembly process.^[37] The increase in turbidity was followed simultaneously in a batch of six cuvettes (containing 1.0 mg mL^{-1} MTP in 0.1 M MES buffer, 1 mM ethylene glycol tetraacetic acid (EGTA), 1 mM MgCl_2 , 1 mM β -ME, 1.5 mM guanosine triphosphate (GTP), pH 6.7, and the measured ligand concentration), with a control (i.e., with no ligand) always being included. The samples were preincubated for 30 min at 20°C to allow binding of the ligand, and were cooled on ice for 10 min. The cuvettes were then placed in the spectrophotometer at 4°C . The assembly process was initiated by a shift in the temperature to 37°C .

Acknowledgements

We thank the Junta de Castilla y León (ref. SA067A09, SA063A09), the Spanish MEC/MICINN (ref. SAF2008-04242) and the EU (Structural Funds) for financial support. C.A. and R.A. thank the Spanish MEC for FPI predoctoral grants.

- [1] a) T. Shen, X.-N. Wang, H.-X. Lou, *Nat. Prod. Rep.* **2009**, *26*, 916–935; b) I. Chrzaszcik, *Crit. Rev. Anal. Chem.* **2009**, *40*, 70–80; c) K. Xiao, H.-J. Zhang, L.-J. Xuan, J. Zhang, Y.-M. Xu, D.-L. Bai, *Stud. Nat. Prod. Chem.* **2008**, *34*, 453–646; d) F. Orsini, G. Sello, *Stud. Nat. Prod. Chem.* **2008**, *34*, 77–127.
- [2] a) R. Singh, H. Kaur, *Synthesis* **2009**, 2471–2491; b) G. C. Tron, T. Pirali, G. Sorba, F. Pagliari, S. Busacca, A. Genazzani, *J. Med. Chem.* **2006**, *49*, 3033–3044.
- [3] a) R. F. Guerrero, M. C. Garcia-Parrilla, B. Puertas, E. Cantos-Villar, *Nat. Prod. Commun.* **2009**, *4*, 635–658; b) F. Orallo, *Curr. Med. Chem.* **2008**, *15*, 1887–1898; c) R. Chillemi, S. Sciuto, C. Spatafora, C. Tringali, *Nat. Prod. Commun.* **2007**, *2*, 499–513; d) F.

- Orallo, *Curr. Med. Chem.* **2006**, *13*, 87–98; e) J. A. Baur, D. A. Sinclair, *Nat. Rev. Drug Discovery* **2006**, *5*, 493–506.
- [4] a) S. Y. Liao, J. C. Chen, T. F. Miao, Y. Shen, K. C. Zheng, *J. Enzyme Inhib. Med. Chem.* **2010**, *25*, 421–429; b) D. Simoni, R. Romagnoli, R. Baruchello, R. Rondanin, M. Rizzi, M. G. Pavani, D. Alloatti, G. Giannini, M. Marcellini, T. Riccioni, M. Castorina, M. B. Guglielmi, F. Bucci, P. Carminati, C. Pisano, *J. Med. Chem.* **2006**, *49*, 3143–3152; c) T. L. Nguyen, C. McGrath, A. R. Hermone, J. C. Burnett, D. W. Zaharevitz, B. W. Day, P. Wipf, E. Hamel, R. Gussio, *J. Med. Chem.* **2005**, *48*, 6107–6116; d) S. Ducki, G. Mackenzie, N. J. Lawrence, J. P. Snyder, *J. Med. Chem.* **2005**, *48*, 457–465.
- [5] a) D. W. Siemann, D. J. Chaplin, P. A. Walicke, *Expert Opin. Invest. Drugs* **2009**, *18*, 189–197; b) A. Gaya, F. Daley, N. J. Taylor, G. Tozer, U. Qureshi, A. Padhani, R. B. Pedley, R. Begent, D. Wellsted, J. J. Stirling, G. Rustin, *Br. J. Cancer* **2008**, *99*, 321–326; c) D. W. Siemann, W. Shi, *Anticancer Res.* **2008**, *28*, 2027–2031; d) D. M. Patterson, G. J. S. Rustin, *Drugs Future* **2007**, *32*, 1025–1032.
- [6] a) S. A. Hill, D. J. Chaplin, G. Lewis, G. M. Tozer, *Int. J. Cancer* **2002**, *102*, 70–74; b) C. J. Mooney, G. Nagaiah, P. Fu, J. K. Wasman, M. M. Cooney, P. S. Savvides, J. A. Bokar, A. Dowlati, D. Wang, S. S. Agarwala, S. M. Flick, P. H. Hartman, J. D. Ortiz, P. N. Lavertu, S. C. Remick, *Thyroid* **2009**, *19*, 233–240; c) D. J. Chaplin, M. R. Horsman, D. W. Siemann, *Curr. Opin. Invest. Drugs* **2006**, *7*, 522–528; d) <http://www.clinicaltrials.gov/ct2/results?term=fosbretabulin>; <http://www.clinicaltrials.gov/ct2/results?term=ZYBRESTAT>; <http://www.oxigene.com/pipeline.php>.
- [7] a) I. Barrett, M. Carr, N. O'Boyle, L. M. Greene, A. J. S. Knox, D. G. Lloyd, D. M. Zisterer, M. J. Meegan, *J. Enzyme Inhib. Med. Chem.* **2010**, *25*, 180–194; b) B. Pandit, Y. Sun, P. Chen, D. L. Sackett, Z. Hu, W. Rich, C. Li, A. Lewis, K. Schaefer, P.-K. Li, *Bioorg. Med. Chem.* **2006**, *14*, 6492–6501; c) C. G. Wermuth in *The Practice of Medicinal Chemistry*, 2nd ed. (Ed.: C. G. Wermuth) Academic Press, London, **2003**, pp. 215–231.
- [8] E. K. Singh, R. P. Sellers, L. D. Alexander, S. R. McAlpine, *Curr. Opin. Drug Discovery Dev.* **2008**, *11*, 544–552.
- [9] a) O. Querolle, J. Dubois, S. Thoret, F. Roussi, F. Guéritte, D. Guénard, *J. Med. Chem.* **2004**, *47*, 5937–5944; b) C. J. Dinsmore, M. J. Bogusky, J. Ch. Culberson, J. M. Bergman, C. F. Homnick, C. Blair Zartman, S. D. Mosser, M. D. Schaber, R. G. Robinson, K. S. Koblan, H. E. Huber, S. L. Graham, G. D. Hartman, J. R. Huff, T. M. Williams, *J. Am. Chem. Soc.* **2001**, *123*, 2107–2108; c) A. K. Ghosh, L. M. Swanson, H. Cho, S. Leshchenko, K. Azhar Hussain, S. Kay, D. E. Walters, Y. Koh, H. Mitsuya, *J. Med. Chem.* **2005**, *48*, 3576–3585; d) X. Hu, K. T. Nguyen, V. C. Jiang, D. Lofland, H. E. Moser, D. Pei, *J. Med. Chem.* **2004**, *47*, 4941–4949.
- [10] S. Bartlett, G. S. Beddard, R. M. Jackson, V. Kayser, C. Kilner, A. Leach, A. Nelson, P. R. Oledzki, P. Parker, G. D. Reid, S. L. Warriner, *J. Am. Chem. Soc.* **2005**, *127*, 11699–11708, and references therein.
- [11] Y. Kim, M. A. Arai, T. Arai, J. O. Lamenzo, E. F. Dean, N. Patterson, P. A. Clemons, S. L. Schreiber, *J. Am. Chem. Soc.* **2004**, *126*, 14740–14745.
- [12] a) C. Mateo, C. Perez-Melero, R. Peláez, M. Medarde, *Tetrahedron Lett.* **2005**, *46*, 7055–7057; b) C. Mateo, C. Perez-Melero, R. Peláez, M. Medarde, *J. Org. Chem.* **2005**, *70*, 6544–6547; c) C. Mateo, R. Alvarez, C. Perez-Melero, R. Peláez, M. Medarde, *Bioorg. Med. Chem. Lett.* **2007**, *17*, 6316–6320; d) C. Mateo, V. Lopez, M. Medarde, R. Peláez, *Chem. Eur. J.* **2007**, *13*, 7246–7256.
- [13] a) F. Vögtle, P. Neumann, *Tetrahedron* **1970**, *26*, 5847–5873; b) *Cyclophanes, Vols. 1 and 2* (Eds.: P. M. Keehn, S. M. Rosenfeld), Academic Press, New York, **1983**; c) F. Vögtle, *Cyclophane Chemistry*, Wiley, New York, **1993**; d) *Cyclophanes* (Ed.: E. Weber), Springer, Berlin, **1994**; e) *Modern Cyclophane Chemistry* (Eds.: R. Gleiter, H. Hopf), Wiley-VCH, Weinheim, **2004**; f) L. Ernst, *Annu. Rep. NMR Spectrosc.* **2006**, *60*, 77–143.
- [14] a) H. R. Darabi, M. A. Arani, A. Motamedi, R. Firuzi, R. Herges, A. R. Mohebbi, S. M. Nasser, C. Nather, *Supramol. Chem.* **2009**, *21*, 632–637; b) T. Sawada, M. Morita, K. Chifuku, Y. Kuwahara, H. Shosenji, M. Takafuji, H. Ihara, *Tetrahedron Lett.* **2007**, *48*, 9051–9055; c) J. Gierschner, H. G. Mack, D. Oelkrug, I. Waldner, H. Rau, *J. Phys. Chem. A* **2004**, *108*, 257–263; d) L. Ernst, *Prog. Nucl. Magn. Reson. Spectrosc.* **2000**, *37*, 4–190; e) D. Tanner, O. Wennerstrom, *Tetrahedron Lett.* **1981**, *22*, 2313–2316.
- [15] a) P. Rajakumar, S. Selvam, *Tetrahedron* **2007**, *63*, 8891–8901; b) P. Rajakumar, R. Kanagalatha, *Tetrahedron Lett.* **2007**, *48*, 8496–8500.
- [16] a) P. Rajakumar, M. G. Swaroop, S. Jayavelu, K. Murugesan, *Tetrahedron Lett.* **2006**, *47*, 3019–3022; c) P. Rajakumar, M. G. Swaroop, *Tetrahedron Lett.* **2005**, *46*, 8543–8546; d) P. Rajakumar, M. G. Swaroop, *Tetrahedron Lett.* **2004**, *45*, 6165–6167; e) R. Gibe, J. R. Green, G. Davidson, *Org. Lett.* **2003**, *5*, 1003–1005; f) R. Gibe, J. R. Green, G. Davidson, *Org. Lett.* **2003**, *5*, 1003–1005; g) G. J. Bodwell, J. Li, *Org. Lett.* **2002**, *4*, 127–130.
- [17] a) Lignans: B. Madrigal, P. Puebla, R. Peláez, E. Caballero, M. Medarde, *J. Org. Chem.* **2003**, *68*, 854–864; b) indolocarbazole alkaloids: M. Adeva, H. Sahagun, E. Caballero, R. Peláez, M. Medarde; F. Tomé, *J. Org. Chem.* **2000**, *65*, 3387–3394; c) combretastatins: C. Perez-Melero, A. B. S. Maya, B. del Rey, R. Peláez, E. Caballero, M. Medarde, *Bioorg. Med. Chem. Lett.* **2004**, *14*, 3771–3774; d) combretastatins: A. B. S. Maya, C. Perez-Melero, C. Mateo, D. Alonso, J. L. Fernandez, C. Gajate, F. Mollinedo, R. Peláez, E. Caballero, M. Medarde, *J. Med. Chem.* **2005**, *48*, 556–568; e) isocombretastatins: R. Alvarez, C. Alvarez, F. Mollinedo, B. G. Sierra, M. Medarde, R. Peláez, *Bioorg. Med. Chem.* **2009**, *17*, 6422–6431; f) phenstatins: C. Alvarez, R. Alvarez, P. Corchete, C. Perez-Melero, R. Peláez, M. Medarde, *Bioorg. Med. Chem.* **2008**, *16*, 8999–9008; g) phenstatins: C. Alvarez, R. Alvarez, P. Corchete, C. Perez-Melero, R. Peláez, M. Medarde, *Eur. J. Med. Chem.* **2010**, *45*, 588–597.
- [18] M. Cushman, D. Nagarathnam, D. Gopal, A. K. Chakraborti, C. M. Lin, E. Hamel, *J. Med. Chem.* **1991**, *34*, 2579–2588.
- [19] a) O. Mitsunobu, *Synthesis* **1981**, 1–28; b) D. L. Hughes, *Org. React.* **1992**, *42*, 335–656; c) D. L. Hughes, *Org. Prep. Proced. Eur.* **2006**, *28*, 127–164; d) K. C. Kumara Swamy, N. N. Bhuvan Kumar, E. Balaraman, K. V. P. Pavan Kumar, *Chem. Rev.* **2009**, *109*, 2551–2651.
- [20] a) E. V. Dehmlow, S. S. Dehmlow, *Phase Transfer Catalysis*, 3rd ed., VCH, Weinheim, **1993**; b) C. M. Starks, C. L. Liotta, M. Halpern, *Phase-Transfer Catalysis*, Chapman & Hall, New York, **1994**; c) Y. Sasson, R. Neumann, *Handbook of Phase-Transfer Catalysis*, Blackie Academic & Professional, London, **1997**; d) M. E. Halpern, *Phase-Transfer Catalysis*, ACS Symposium Series 659, ACS, Washington, **1997**; e) R. A. Jones, *Aldrichimica Acta* **1976**, *9*, 35–45; f) A. McKillop, J.-C. Fiaud, R. P. Hug, *Tetrahedron* **1974**, *30*, 1379–1382.
- [21] a) A. R. Tunoori, D. Dutta, G. I. Georg, *Tetrahedron Lett.* **1998**, *39*, 8751–8754; b) J. C. Pelletier, S. Kincaid, *Tetrahedron Lett.* **2000**, *41*, 797–800; c) A. J. Reynolds, M. Kassiou, *Curr. Org. Chem.* **2009**, *13*, 1610–1632; d) R. Dembinski, *Eur. J. Org. Chem.* **2004**, 2763–2772; e) S. Dandapani, D. P. Curran, *Chem. Eur. J.* **2004**, *10*, 3130–3138; f) E. Valeur, D. Roche, *Tetrahedron Lett.* **2008**, *49*, 4182–4185.
- [22] a) R. Shukla, D. M. Brody, S. V. Lindeman, R. Rathore, *J. Org. Chem.* **2006**, *71*, 6124–6129; b) J. E. McMurry, *Chem. Rev.* **1989**, *89*, 1513–1524; c) M. Ephritikhine, C. Villiers, *The McMurry Coupling and Related Reactions in Modern Carbonyl Olefination: Methods and Applications* (Ed.: T. Takeda), Wiley-VCH, New York, **2004**; d) T. Kawase, N. Ueda, K. Tanaka, Y. Seirai, M. Oda, *Tetrahedron Lett.* **2001**, *42*, 5509–5511.
- [23] a) T. Mukaiyama, T. Sato, J. Hanna, *Chem. Lett.* **1973**, 1041–1044; b) J. E. McMurry, J. G. Rico, *Tetrahedron Lett.* **1989**, *30*, 1169–1172; c) T. Li, W. Cui, J. Liu, J. Zhao, Z. Wang, *Chem. Commun.* **2000**, 139–140; d) A. Gansäuer, *Synlett* **1997**, 363–364; e) F. T. Ladipo, *Curr. Org. Chem.* **2006**, *10*, 965–980; f) A. Gansäuer, H. Bluhm, *Chem. Rev.* **2000**, *100*, 2771–2788; g) X. F. Duan, J. X. Feng, G. F. Zi, Z. B. Zhang, *Synthesis* **2009**, 277–282.
- [24] a) G. M. Robertson, *Comprehensive Organics Synthesis: Carbon-Carbon σ -Bond Formation*, Pergamon Press, New York, **1991**, 563–611; b) T. A. Lipski, A. Hilfiker, S. G. Nelson, *J. Org. Chem.* **1997**, *62*, 4566–4567.

- [25] Conformational studies on combretastatins have been carried with different members of this family: a) L. Padmaja, C. Ravikumar, D. Sajan, I. H. Joe, V. S. Jayakumar, G. R. Pettit, O. F. Nielsen, *J. Raman Spectrosc.* **2009**, *40*, 419–428; b) D. Sajan, J. P. Abraham, I. Hubert Joe, V. S. Jayakumar, J. Aubard, O. Faurskov Nielsen, *J. Mol. Struct.* **2008**, *889*, 129–143; c) C. James, G. R. Pettit, O. F. Nielsen, V. S. Jayakumar, I. Hubert Joe, *Spectrochim. Acta Part A* **2008**, *70*, 1208–1216; d) S. Kim, S. Y. Min, S. K. Lee, W.-J. Cho, *Chem. Pharm. Bull.* **2003**, *51*, 516–521.
- [26] a) Z. Rappoport, S. E. Biali, *Acc. Chem. Res.* **1997**, *30*, 307–314; b) E. Gur, M. Kaftory, S. E. Biali, Z. Rappoport, *J. Org. Chem.* **1999**, *64*, 8144–8148.
- [27] The preferred helical disposition of *cis*-stilbene in the ground state has been often described: a) D. Yusheng, R. E. Allen, *J. Chem. Phys.* **2003**, *119*, 10658–10666; b) R. Improta, F. Santoro, *J. Phys. Chem. A* **2005**, *109*, 10058–10067; c) V. Molina, M. Merchán, B. O. Roos, *Spectrochim. Acta* **1999**, *55*, 433–446; d) G. Hohlneicher, M. Muller, M. Demmer, J. Lex, J. H. Penn, L.-X. Can, P. D. Loesell, *J. Am. Chem. Soc.* **1988**, *110*, 4483–4494.
- [28] a) F. Momicchioli, I. Baraldi, M. C. Bruni, *Chem. Phys.* **1982**, *70*, 161–176; b) J. Almlöf, *Chem. Phys.* **1974**, *6*, 135; c) A. Wolf, H. H. Schmidtke, J. V. Knop, *Theor. Chim. Acta* **1978**, *48*, 37–45.
- [29] Systematic conformational searches by using Monte Carlo and MM2 and MM3 molecular force fields were performed with MacroModel v. 5.1 and clustering of the resulting conformations with XCluster on Silicon Graphics workstations.
- [30] Line-shape analysis of the mutual exchange for the methoxy and aromatic signals of **18a** gave reasonably good simulations with an activation enthalpy of about 10 kcalmol⁻¹. The simulations were carried out with the following program: g-NMR v.5.0.6.0, Ivory soft, Bethesda, MD, **2006**. These results are in good agreement with theoretical calculations.
- [31] The limited water solubility of the compounds did not allow us to calculate IC₅₀ values.
- [32] R. B. Ravelli, B. Gigant, P. A. Curmi, I. Jourdain, S. Lachkar, A. Sobel, M. Knossow, *Nature* **2004**, *428*, 198–202.
- [33] A. Dorleans, B. Gigant, R. B. Ravelli, P. Mailliet, V. Mikol, M. Knossow, *Proc. Natl. Acad. Sci. USA* **2009**, *106*, 13775–13779.
- [34] M. L. Shelanski, F. Gaskin, C. R. Cantor, *Proc. Natl. Acad. Sci. USA* **1973**, *70*, 765–768.
- [35] C. Dumortier, M. Gorbunoff, J. M. Andreu, Y. Engelborghs, *Biochemistry* **1996**, *35*, 4387–4395.
- [36] M. M. Bradford, *Anal. Biochem.* **1976**, *72*, 248–254.
- [37] Y. Han, A. G. Chaudhary, M. D. Chordia, D. L. Sackett, B. Pérez-Ramírez, D. G. Kingston, S. Bane, *Biochemistry* **1996**, *35*, 14173–14183.
- [38] CCDC-813154 contains the supplementary crystallographic data for this paper. These data can be obtained free of charge from The Cambridge Crystallographic Data Centre via www.ccdc.cam.ac.uk/data_request/cif.

Received: October 5, 2010
Published online: February 23, 2011